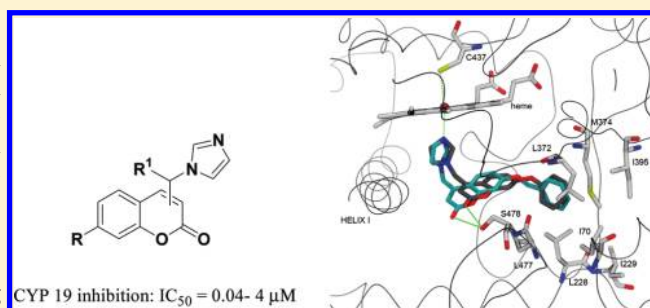


Design, Synthesis, and Biological Evaluation of Imidazolyl Derivatives of 4,7-Disubstituted Coumarins as Aromatase Inhibitors Selective over 17- α -Hydroxylase/C17–20 LyaseAngela Stefanachi,[†] Angelo D. Favja,[†] Orazio Nicolotti,[†] Francesco Leonetti,[†] Leonardo Pisani,[†] Marco Catto,[†] Christina Zimmer,[§] Rolf W. Hartmann,[§] and Angelo Carotti^{*,†}[†]Dipartimento Farmaco-Chimico, Università degli Studi di Bari "Aldo Moro", via Orabona 4, I-70125 Bari, Italy[‡]D3 Department, Istituto Italiano di Tecnologia (IIT), via Morego 30, I-16163 Genoa, Italy[§]Pharmaceutical and Medicinal Chemistry, Saarland University & Helmholtz Institute for Pharmaceutical Research Saarland (HIPS), P.O. Box 15 11 50, D-66041 Saarbrücken, Germany

ABSTRACT: The design, synthesis, and biological evaluation of a series of new aromatase (AR, CYP19) inhibitors bearing an imidazole ring linked to a 7-substituted coumarin scaffold at position 4 (or 3) are reported. Many compounds exhibited an aromatase inhibitory potency in the nanomolar range along with a high selectivity over 17- α -hydroxylase/C17–20 lyase (CYP17). The most potent AR inhibitor was the 7-(3,4-difluorophenoxy)-4-imidazolylmethyl coumarin **24** endowed with an IC_{50} = 47 nM. Docking simulations on a selected number of coumarin derivatives allowed the identification of the most important interactions driving the binding and clearly indicated the allowed and disallowed regions for appropriate structural modifications of coumarins and closely related heterocyclic molecular scaffolds.



INTRODUCTION

Seventy-five percent of breast cancers in postmenopausal women are estrogen-dependent (ER^+).¹ While in premenopausal women estrogens are principally produced by ovaries, during postmenopause, they continue to be synthesized by nonovarian tissues,² such as breast tissue.³ This peripheral synthesis allows estrogens to reach locally a concentration 4–6 times higher than in the serum and equivalent to breast tissue levels recorded in premenopausal women.^{4,5}

Estrogens are biosynthesized from circulating androgens through an aromatization reaction of the steroidal A ring, catalyzed by the enzyme aromatase (AR, CYP19). Because in malignant tissues AR activity and estrogen levels are higher than in healthy tissues, two main strategies have been devised by medicinal chemists to control or block the pathological activity in ER^+ cancer.⁶

The first one implies the block of the binding of estrogens to their biological receptor, the estrogen receptor (ER), with antagonists⁷ among which tamoxifen and raloxifen have proven to be very effective drugs in the treatment of breast cancer.⁸ Unfortunately, in some tissues, such as the uterus and vasculature, such compounds also present an estrogenic action, less pronounced with raloxifen,⁹ and this results in an increased risk of endometrial cancer¹⁰ and stroke.¹¹ Hence, more selective estrogen receptor modulators (SERMs) are eagerly pursued.¹² Furthermore, a second strategy was devised by directly targeting AR, a key enzyme in the biosynthesis of estrogens. Aromatase inhibitors (ARIs), acting on the estrogen biosynthesis, present

fewer side effects than ER antagonists because of the lack of estrogenic activity on uterus and vasculature.¹³

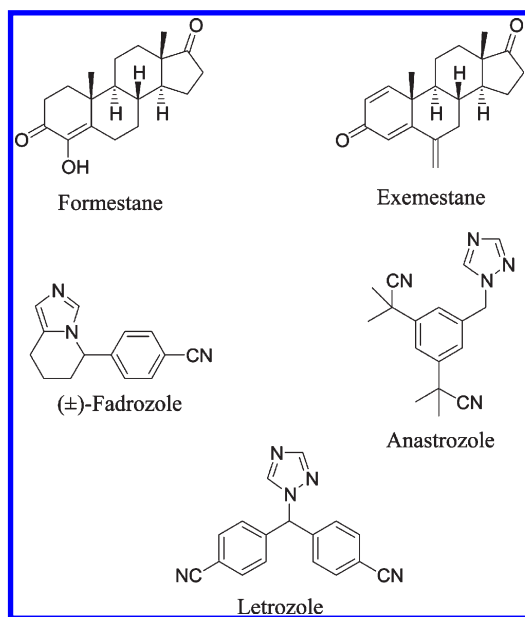
Localized in the endoplasmic reticulum of cells, AR is a multienzymatic complex consisting of two main components, a form of cytochrome P450 (CYP19) and a NADPH-cytochrome P450 flavoprotein reductase. AR catalyzes the conversion of androgens to estrogens through the transformation of the steroidal enone A ring into the aromatic phenolic ring with the concomitant loss of the C19 methyl group.^{14–17} The earliest ARIs were discovered in the early 1970s, and formestane (Chart 1) was the first selective ARI approved for the treatment of breast cancer. Nowadays, exemestane, whose structure closely resembles that of formestane (Chart 1), anastrozole and letrozole, both sharing a nonsteroidal 1,2,4-triazolyl structure, have been approved by FDA.^{18–20} The effectiveness of the triazolyl inhibitors in blocking the enzymatic activity resides in their ability to coordinate the iron atom of the AR heme group by means of the lone pair carried on the triazole nitrogen at position 4. Anastrozole and letrozole have been recommended by the FDA as first-line drugs in the therapy of breast carcinoma.²¹

Despite their selectivity, the prolonged clinical use of ARIs eventually leads to severe side effects, arising mainly from the concomitant, unwanted inhibition of other CYP enzymes, and

Received: August 30, 2010

Published: February 22, 2011

Chart 1. Chemical Structures of Some ARIs



this calls for new, potent, more selective, and less toxic CYP19 inhibitors.^{22–29} Along this research line, we have begun a systematic, long-term study, aiming at the design and synthesis of new ARIs endowed with improved biological, pharmacological, and toxicological profiles. Our first study dealing with the design, synthesis, and biological evaluation as CYP19 inhibitors of a series of 4-imidazolylmethyl-7-substituted coumarins was reported in 2004³⁰ followed by the publication at the wwPDB³¹ of a three-dimensional homology model of the human AR enzyme³² later used as a valuable tool for structure-based ligand design.^{27,33,34}

Biological and modeling results from these two papers^{30,32} suggested 4-imidazolylmethyl-7-substituted coumarin derivatives **1** and **14** (Table 1) as promising leads for further structural modifications aimed to deepen our understanding of structure–affinity relationships (SAFIRs) and to discover new molecules with potent AR inhibition along with good selectivity over 17- α -hydroxylase/C17–20 lyase (CYP17) and therapeutic potential in breast cancer. CYP17 is a cytochrome P450-dependent enzyme, involved in the development of prostatic cancer, and huge efforts are currently devoted to the synthesis of selective CYP17 enzyme inhibitors, which may halt the progression of this tumor toward pharmacologically untreatable advanced forms.^{35–37}

Developing molecules that act selectively toward one of the two strictly related CYP17 and CYP19 enzymes represents nowadays a very important task for medicinal chemists and may constitute a logical follow up of the present work.

Starting from the remarkable AR inhibitory activity and CYP19 over CYP17 selectivity exhibited by compounds **1** and **14**, two new series of coumarin derivatives, **2–13** and **15–26** (Table 1), were designed, prepared, and tested to explore the substituent effects on the 7-benzyloxy and 7-phenoxy aromatic rings, respectively. Moreover, the synthesis of derivatives **28–32** (Table 1) was also undertaken to analyze the effect on affinity and selectivity resulting from the introduction of a phenyl and substituted phenyl rings on the 4-methylene bridge of lead compound **14**. Eventually, 3-substituted

coumarin **34** was designed to verify the importance of a regioselective interaction within the AR binding site. In this regard, all of the designed inhibitors might also serve as valuable molecular probes to gain insights into main structural features of the binding site regions of AR.

In addition, the recently solved crystal structure of human AR^{38,39} was exploited to better rationalize the outcomes of the biological assays. To this aim, docking simulations of selected ligands were performed on a suitable refined model of the enzyme to reproduce likely induced fit phenomena occurring upon binding. The analysis of their putative binding conformations helped to shed light on the key structural features responsible for high inhibitory potencies.

CHEMISTRY

Compounds **1–13** (Scheme 1) were synthesized from 4-chloromethyl-7-hydroxycoumarin,^{30,40} through the benzylation of its phenolic group followed by the nucleophilic substitution of the chlorides with imidazole. Compound **26** was obtained directly from 4-chloromethyl-7-hydroxycoumarin by a nucleophilic substitution with imidazole. As described in Scheme 1, for the synthesis of compounds **14–24**, the phenolic group was first arylated by a copper acetate-mediated coupling,⁴¹ and then, the imidazole ring was introduced, as above.

The synthesis of compound **25** (Scheme 2) started with the von Pechmann reaction between (3-hydroxyphenyl)carbamic acid ethyl ester intermediate **25a**⁴² and ethyl 4-chloroacetoacetate. After deprotection, the amino group was arylated by a copper acetate-mediated coupling,⁴³ and then, final compound **25** was obtained by a nucleophilic substitution reaction with imidazole.

To obtain compound **28** (Scheme 3), 4-benzyl-7-hydroxycoumarin **28a**⁴⁴ was methylated by CH₃I and NaH in DMF, brominated by *N*-bromosuccinimide (NBS) in CCl₄, and reacted with imidazole.

Intermediates **29b**, **31b**, and **32b** (Scheme 4) were obtained by von Pechmann cyclocondensation of 3-phenoxyphenol with the corresponding ethyl phenylacetoacetates **29a**, **31a**, and **32a**, respectively.⁴⁵ As before, methylene bromination with NBS followed by reaction with imidazole yielded the desired final compounds **29**, **31**, and **32**.

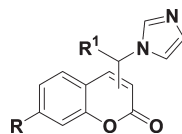
The synthesis of compound **30** (Scheme 5) started with the arylation of the phenolic intermediate **28a** followed by methylene bromination and reaction with imidazole.

The synthesis of compound **34** (Scheme 6), a 3,7-disubstituted coumarin derivative, was accomplished starting from intermediate **34a**,⁴⁶ which was demethylated by BBr₃, arylated by a copper acetate-mediated coupling, and brominated by NBS in CCl₄. The subsequent nucleophilic substitution with imidazole gave compound **34**.

BIOLOGICAL ASSAYS

All of the molecules in Table 1 were tested for their inhibitory activities against AR (CYP19) and 17 α -hydroxylase/C17,20-lyase (CYP17), two related P450 enzymes, which are responsible for catalyzing the final step in estrogen and androgen biosynthesis, respectively. In the case of CYP19, human placental microsomes were used as a source of the enzyme and [1 β -³H] androstenedione as a substrate as described by Thompson and Siiteri,¹⁴ with slight modifications.^{47,48} For the determination of CYP17 inhibition, microsomes from *Escherichia coli*-expressing human CYP17 and progesterone as substrate were applied;^{48,49}

Table 1. Chemical Structures and Inhibition Data of Coumarin Derivatives 1–34



entry	R	R ^{1a}	CYP19 inhibition ^b	CYP17 inhibition ^c (%)
1 ³⁰	C ₆ H ₅ CH ₂ O	H	0.150	3
2	3'-CH ₃ C ₆ H ₄ CH ₂ O	H	0.114	0
3	3'-FC ₆ H ₄ CH ₂ O	H	0.113	0
4	3'-ClC ₆ H ₄ CH ₂ O	H	0.130	3
5	3'-CF ₃ C ₆ H ₄ CH ₂ O	H	0.235	0
6	3'-OCF ₃ C ₆ H ₄ CH ₂ O	H	0.207	3
7	3'-NO ₂ C ₆ H ₄ CH ₂ O	H	0.141	3
8	4'-FC ₆ H ₄ CH ₂ O	H	0.267	0
9	4'-ClC ₆ H ₄ CH ₂ O	H	0.178	1
10	4'-OCH ₃ C ₆ H ₄ CH ₂ O	H	0.127	0.5
11	4'-OCF ₃ C ₆ H ₄ CH ₂ O	H	0.481	0.5
12	3',5'-F ₂ C ₆ H ₃ CH ₂ O	H	0.169	2
13	3',4'-F ₂ C ₆ H ₃ CH ₂ O	H	0.165	1
14 ³⁰	C ₆ H ₅ O	H	0.051	26
15	3'-FC ₆ H ₄ O	H	0.072	1
16	3'-ClC ₆ H ₄ O	H	0.072	2
17	3'-OCH ₃ C ₆ H ₄ O	H	0.292	2
18	4'-CH ₃ C ₆ H ₄ O	H	0.690	1
19	4'-ClC ₆ H ₄ O	H	0.112	5
20	4'-CNC ₆ H ₄ O	H	0.164	16
21	4'-COCH ₃ C ₆ H ₄ O	H	0.296	4
22	4'-N(CH ₃) ₂ C ₆ H ₄ O	H	0.081	3
23	3',5'-F ₂ C ₆ H ₃ O	H	0.070	1
24	3',4'-F ₂ C ₆ H ₃ O	H	0.047	14
25	C ₆ H ₅ NH	H	0.105	3
26	HO	H	3.75	7
27 ³⁰	CH ₃ O	H	0.280	14
28	CH ₃ O	C ₆ H ₅	0.455	3
29	C ₆ H ₅ O	C ₆ H ₅	0.067	4
30	3',4'-F ₂ C ₆ H ₃ O	C ₆ H ₅	0.317	1
31	C ₆ H ₅ O	4-ClC ₆ H ₄	0.532	5
32	C ₆ H ₅ O	4-CNC ₆ H ₄	4.01	3
33 ^{d30}	CH ₃ O	H	2.82	43
34 ^d	C ₆ H ₅ O	C ₆ H ₅	0.313	13

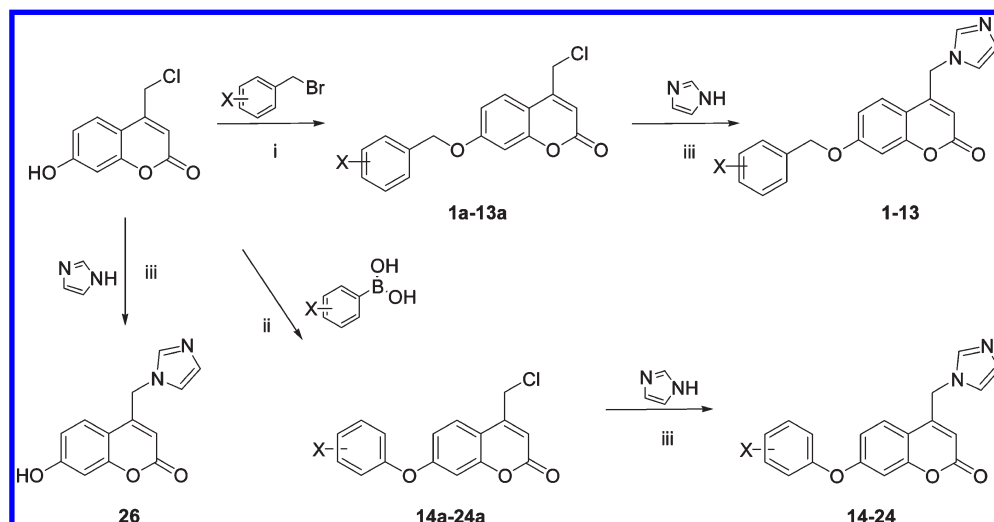
^a Chiral compounds carrying a phenyl substituent on the methylene bridge at position 4 or 3 were tested as racemic mixtures. ^b IC₅₀ values (μM) coming from three independent experiments; the SEMs were always <10%; substrate, 500 nM 1β-³H androstenedione/androstenedione. ^c Percent at 2.5 μM; substrate, 25 μM progesterone; enzyme, bacterial membranes containing recombinantly expressed human CYP17; reference compounds, 1. IC₅₀, 0.15 μM for CYP19; ketoconazole IC₅₀, 4.5 μM for CYP17. ^d Compounds 33 and 34 are 3-substituted coumarin derivatives.

the inhibition data are shown in Table 1 as a percentage of inhibition at the indicated concentration. Compounds 1 and 24 also were tested as inhibitors of the two enzymes catalyzing the final step of corticosteroids biosynthesis, namely, CYP11B1,⁵⁰ for cortisol and CYP11B2^{51–54} for aldosterone. The assay was carried out on V79MZ cells expressing human CYP11B1 and CYP11B2 genes by using [1,2-³H]11-deoxycorticosterone/11-deoxycorticosterone as the radioactive substrate; the inhibition data are reported in Table 2.

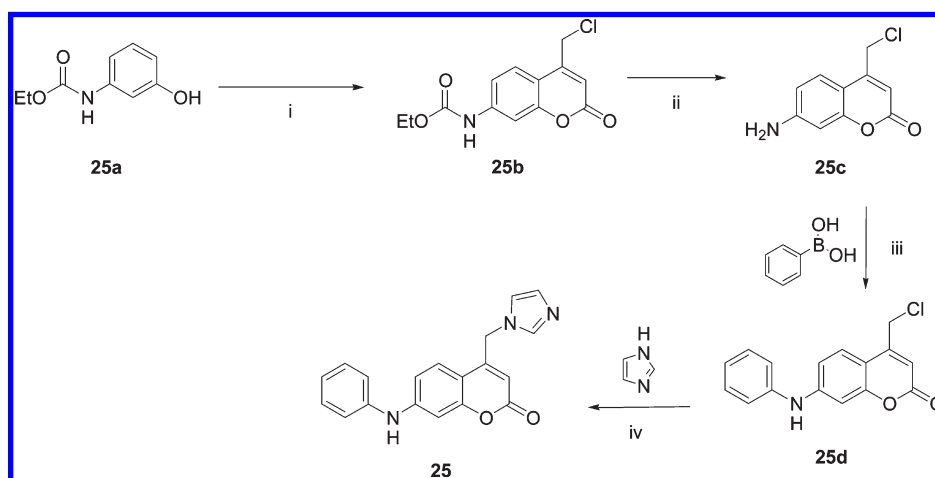
RESULTS AND DISCUSSION

Chemical structures and inhibition data of the newly synthesized and others already described molecules, used herein as reference (i.e., 1, 14, 27, and 33), are reported in Table 1. Inhibition data were expressed as IC₅₀ (μM) for CYP19 and as percentage of inhibition at a 2.5 μM concentration for CYP17.

At a glance, biological data reported in Table 1 indicated that all of the designed compounds showed a very high CYP19/CYP17 selectivity. In fact, the percentage of CYP17 inhibition at

Scheme 1^a

^a Reagents and conditions: (i) K_2CO_3 , EtOH, reflux, 3 h. (ii) $Cu(OAc)_2$, Et_3N , molecular sieves 4 Å, CH_2Cl_2 , room temperature, 18 h. (iii) K_2CO_3 , THF, reflux, 5–7 h.

Scheme 2^a

^a Reagents and conditions: (i) Ethyl 4-chloroacetate, H_2SO_4 70%, room temperature, 4 h. (ii) H_2SO_4 96%, glacial acetic acid, reflux, 4 h. (iii) $Cu(OAc)_2$, Et_3N , CH_2Cl_2 , room temperature, 72 h. (iv) K_2CO_3 , THF, reflux, 5–7 h.

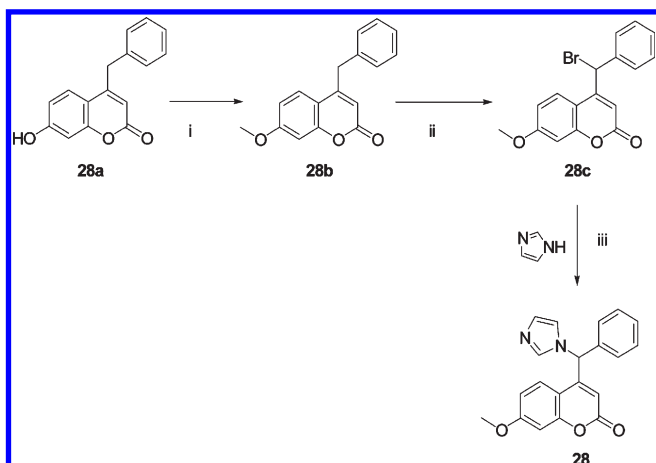
2.5 μM concentration was generally lower than 10%, with very few exceptions. Conversely, IC_{50} values lower than 0.30 μM were exhibited at CYP19 by most of the new compounds.

To gain clear insights into the SAFIRs, data in Table 1 were examined taking into account separately the two homologous series of 7-benzyloxy-4-imidazolylmethylcoumarin derivatives 2–13 and 7-phenoxy-4-imidazolylmethylcoumarin derivatives 15–24. The already reported highly potent inhibitors 1 and 14 were taken as reference compounds for the evaluation of the SAFIRs of the 7-benzyloxy and 7-phenoxy series, respectively.

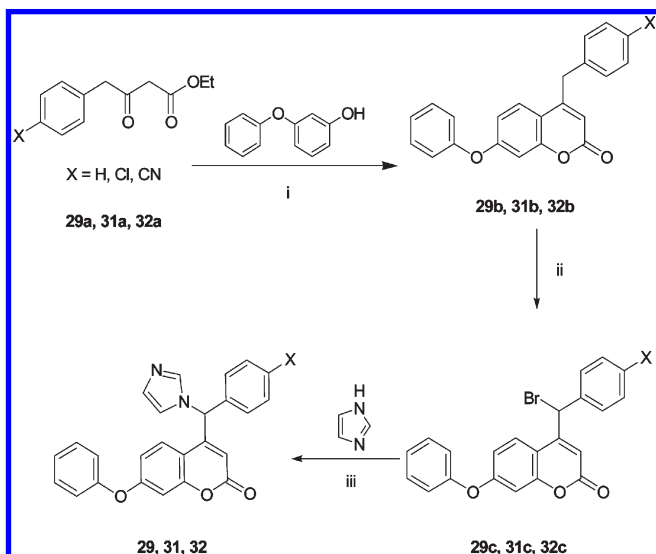
Inhibition data of the 7-benzyloxy derivatives 2–13 fell in the 0.113–0.481 μM range. In comparison with reference compound 1, meta-substituted derivatives 2, 3, and 4 and the para-substituted derivative 10 showed a slightly increased affinity. Para-substituted derivatives are less active than the corresponding meta-substituted analogues (compare 8 vs 3, 9 vs 4, and 11 vs 6), and this may be indicative of a reduced enzymatic accessibility for substituents in that

position. Indeed, compound 11 bearing the larger substituent at the para position was the least potent compound of the 7-benzyloxy series. The 3,5- and 3,4-difluorobenzyloxy derivatives 12 and 13 displayed a slightly weaker activity than reference compound 1. Unfortunately, no clear SAFIR emerged from the analysis of the electronic, hydrophobic, and steric substituent effects of 7-benzyloxy derivatives 1–13.

Inhibition data of the 7-phenoxy derivatives 15–24 fell in the 0.047–0.690 μM range, and only one compound, that is, the 3,4-difluorophenoxy derivative 24, exhibited an inhibitory potency equal or slightly better than the reference compound 14 (0.047 vs 0.051 μM). Similarly to what was observed in the 7-benzyloxy series, the meta-chloro congener 16 exhibited an inhibitory potency higher than the corresponding para derivative 19. Also, for the series of 7-phenoxy coumarin derivatives, no clear electronic, hydrophobic, and steric effects on the affinity could be detected. In fact, the almost isophilic compounds 18

Scheme 3^a

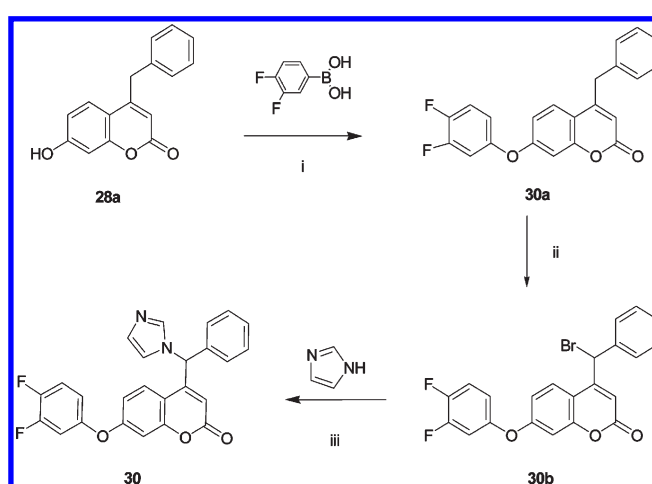
^a Reagents and conditions: (i) NaH, CH₃I, DMF, 0 °C, 1 h. (ii) NBS, DBP, CCl₄, reflux, 1 h. (iii) K₂CO₃, THF, reflux, 7 h.

Scheme 4^a

^a Reagents and conditions: (i) H₂SO₄ 96%, 120 °C, 30 min. (ii) NBS, DBP, CCl₄, reflux, 1 h. (iii) K₂CO₃, THF, reflux, 5–7 h.

and **19** showed a striking different affinity, and the same consideration holds when comparing the affinity of inhibitors **18** and **22**, bearing Me and N(Me)₂ substituents of comparable electron donor ability ($\sigma_p^- = -0.15$ and -0.12 , respectively).⁵⁵ However, it is worth noting that inhibitors carrying halogen substituents in the para and/or meta position (i.e., **15**, **16**, **19**, **23**, and **24**) exhibited the highest affinity within the whole 7-phenoxy series. Despite its hydrophobic character, the introduction of a para-methyl substituent on lead compound **14** determined a dramatic drop of affinity, with compound **18** being the weakest ligand of the 7-phenoxy coumarin series. No sound explanation could be provided to interpret this unexpected result.

The favorable effect of lipophilic substituents at position 7 was quite evident when comparing the affinity of the 7-OH (**26**, IC₅₀ = 3.75 μM), 7-OMe (**27**, IC₅₀ = 0.280 μM), and 7-OPh (**14**, IC₅₀ = 0.051 μM) derivatives. However, the good affinity (IC₅₀ = 0.105 μM)

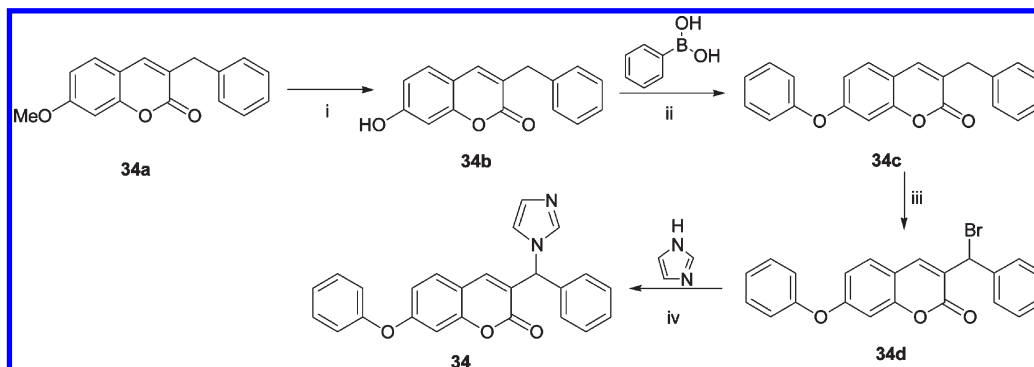
Scheme 5^a

^a Reagents and conditions: (i) Cu(OAc)₂, Et₃N, molecular sieves 4 Å, CH₂Cl₂, room temperature, 4 h. (ii) NBS, DBP, CCl₄, reflux, 4 h. (iii) CH₃CN, reflux, 6 h.

also observed for compound **25** that carries a 7-anilino substituent much more hydrophilic than the 7-phenoxy isosteric substituent of **14** (hydrophobic substituent constant $\pi = 2.08$ and 1.37 , respectively)⁵⁵ suggested that beside the substituent lipophilicity, a conserved binding topology, likely placing the two phenyl rings in similar enzymatic pockets, also plays a key role in the ligand binding process.

To extend the SAFIRs to other regions of the enzyme, a phenyl group was introduced on the methylene bridge at position 4 of lead compound **14**. This structural modification left the affinity nearly unchanged (**29**, IC₅₀ = 0.067 μM vs IC₅₀ = 0.051 μM of **14**). The good affinity of compound **29** and the presence of a chiral center on its 4-substituent prompted us to explore possible enantioselective interactions at the AR active site by measuring the individual activity of the two separated enantiomers. Initially, the separation of the enantiomers of **29** was investigated by using amylose and cellulose packed columns, as well as glycopeptide antibiotics-based stationary phases.⁵⁶ The best enantiomeric separation was obtained on a Chiralpak IA column by using MeOH as the mobile phase ($\alpha = 1.6$, $R_s = 2.0$). Regrettably, the strong acidity of the 4-methylene proton caused a rapid racemization of both of the separated pure enantiomers in solution, and this precluded the execution of any enzymatic inhibition assay. Docking simulations following these discouraging results suggested similar binding energies for the top-scoring poses of the two enantiomers of inhibitor **29**.

The introduction of two fluorine atoms at 3- and 4-positions on the 7-phenoxy ring of **29** led to a 5-fold decrease of affinity (**30**, IC₅₀ = 0.317 μM), and this might indicate either some steric clash or the overcome of some molecular lipophilicity limit. The same explanation might apply to interpret the higher decrease of affinity (IC₅₀ from 0.067 to 0.532 μM) resulting from the introduction of a para-chloro substituent on the 4-benzylic moiety of **29**, resulting in inhibitor **31**. The even more dramatic drop of affinity observed in the para-cyanophenyl derivative **32** seemed to indicate a more likely steric effect at the para position, with the cyano substituent much less lipophilic than chlorine ($\pi = -0.57$ vs 0.71).⁵⁵ The affinity decrease, more evident for the para-cyano congener **32** than for the para-chloro congener **31**, might be ascribed to a different steric effect arising from the two differently shaped substituents.

Scheme 6^a

^a Reagents and conditions: (i) BBr_3 , CH_2Cl_2 , $0^\circ\text{C} \rightarrow$ room temperature, 18 h. (ii) $\text{Cu}(\text{OAc})_2$, Et_3N , molecular sieves 4 \AA , CH_2Cl_2 , room temperature, 1 h. (iii) NBS, DBP, CCl_4 , reflux, 4 h. (iv) CH_3CN , reflux, 6 h.

Table 2. Inhibition Data of Coumarin Derivatives **1** and **24** on the Indicated CYPs

entry	CYP19 inhibition ^a	CYP17 inhibition ^b (%)	CYP11B1 inhibition ^c	CYP11B2 inhibition ^c
1	0.150	3	0.072	0.289
24	0.047	14	0.933	2.19
(±)-fadrozole	0.052	2	0.010	0.001

^a IC_{50} values (μM) coming from 3 independent experiments; the SEM were always $<10\%$; substrate: 1β - ^3H androstenedione/androstenedione 500 nM.

^b % at $2.5 \mu\text{M}$; substrate: progesterone $25 \mu\text{M}$; enzyme: bacterial membranes containing recombinantly expressed human CYP17; ^c IC_{50} values (μM) coming from 3 independent experiments; the SEM were always $<15\%$; substrate: $[1,2\text{-}^3\text{H}]11$ -deoxycorticosterone/11-deoxycorticosterone, 100 nM.

To shed light on the structural determinants responsible for some of the recorded activity variation, compounds **1**, **14**, and **29** were docked at the binding site of the recently solved model of human AR.^{38,39} To overcome the well-known flexibility-related issues given by the use of a single protein structure,⁵⁷ the AR model was subjected to a focused minimization protocol similar in spirit to the ones recently reported by others.^{58,59} As observed for many CYP inhibitors, the binding driving interaction was the heme iron coordination that, for the studied compounds, was mediated by the electron-rich nitrogen of the imidazole ring.

As it can be inferred from Figure 1A, where the putative binding modes of lead compounds **1** and **14** are shown, the coumarin scaffolds were almost perpendicular to the plane of the imidazole ring and stabilized by one hydrogen bond (HB) between the lactone carbonyl and the hydroxyl of S478. In addition, a convenient allocation of the phenoxy and benzyloxy groups in a hydrophobic accessory site constituted of I70, L228, I229, L372, M374, I395, and L477 may be observed. This three-site interaction seemed to be better fulfilled when the coumarin ring carried at position 4 an imidazolylmethyl group and a phenoxy substituent at position 7, and this may justify the better affinity of compound **14** as compared to **1**. Indeed, the longer benzyloxy group at position 7 seemed to induce some modification of the heme coordination and of the HBs pattern. In particular, the distance between the imidazole nitrogen and the lactone carbonyl in both series of compounds is likely to play a major role in the affinity regulation. This hypothesis was fully corroborated by the fact that when the phenyl-imidazolylmethyl substituent was moved to position 3 of the coumarin ring, a substantial affinity drop was observed (compare compound **29** with **34**). The effects of a substitution on the methylene bridge at position 4 could be less easily rationalized due to the lack of inhibition data on separated enantiomers.

However, the investigated binding poses of this class of molecules, illustrated in Figure 1B, where compound **29** is shown as a prototypical case, indicated that both enantiomers bind in a similar fashion, consistent with the above illustrated three-site binding hypothesis. In addition, a local displacement of some amino acids at the bottom of the binding area was needed to allocate correctly the ligand. The nonspecific interactions occurring between the phenyl group of the ligand and the hydrophobic side chains of the protein seem to compensate for the imperfect heme coordination (more pronounced for the *S*-enantiomer), resulting in an IC_{50} value comparable with that of its achiral precursor **14**. Furthermore, the drop of affinity observed upon substitution on the phenyl ring (i.e., **31**) can be ascribed to a restricted accessibility of the active site to that position as well as to the induced changes in the electronic features of the aromatic ring, thus limiting an effective binding. This effect was even more pronounced when a longer and more hydrophilic group such as the cyano substituent was present (i.e., **32**), although in such a case also the suboptimal allocation of the group in a region defined mostly by hydrophobic or negatively charged amino acids (i.e., F134, F221, W224, I305, and D309) was likely to play a significant role.

To evaluate the selectivity of our ARIs over other CYPs involved in the biosynthesis of steroids, one representative compound from both series (i.e., compounds **1** and **24** from the 7-benzyloxy and 7-aryloxy series) was selected and tested toward CYP11B1 (steroid 11β -hydroxylase) and CYP11B2 (aldosterone synthase; Table 2). Interestingly, these enzymes could also be targets for the treatment of Cushing's syndrome or metabolic disease (CYP11B1)⁵⁰ as well as for hyperaldosteronism, congestive heart failure, and myocardial fibrosis (CYP11B2).^{51–54} On the other hand, it is worth noting that an unselective inhibition of these two CYPs by ARIs also could lead to unwanted side effects such as hyponatremia, hyperkalemia, adrenal hyperplasia, and hypovolemic shock.

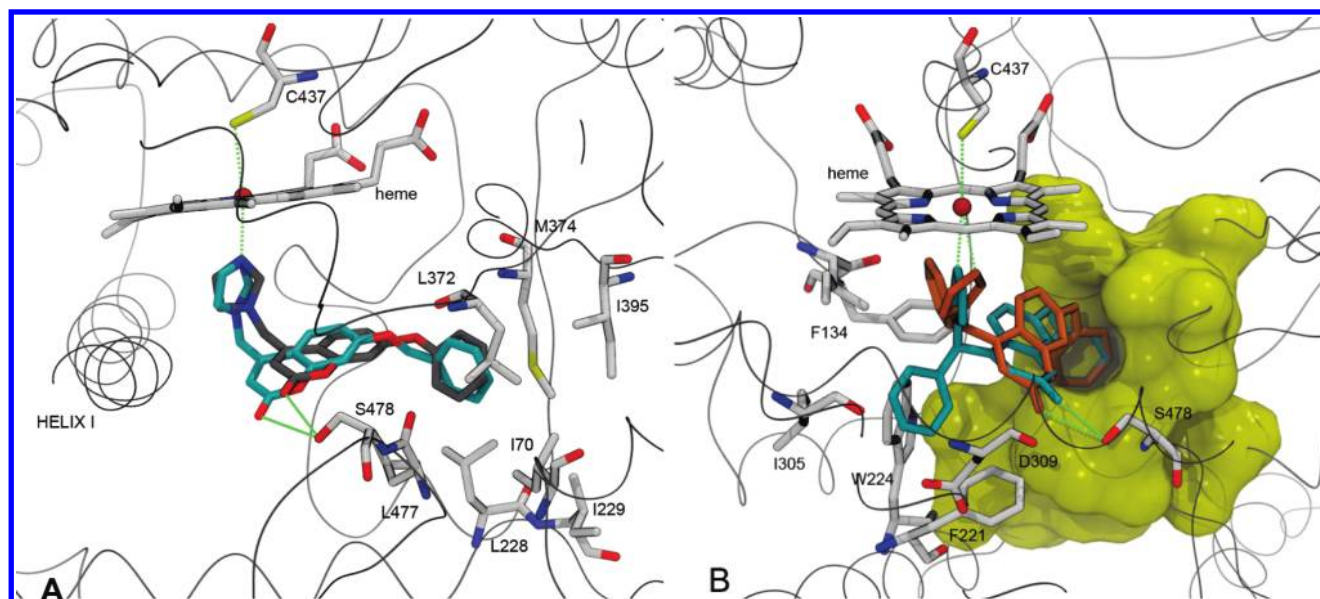


Figure 1. (A) Putative binding mode of compounds **1** and **14** at the enzyme binding site, shown as stick models C-colored gray and cyan, respectively. Helix I of the enzyme is highlighted to help interpretation. (B) Binding models of the two enantiomers of compound **35** at AR active site. The *R*- and *S*-enantiomers are colored cyan and orange, respectively. The yellow blob represents the vdW surface of the aminoacids highlighted in A, not including C437. In both figures, the protein backbone is depicted as ribbons, the green dashed lines are drawn between the atoms likely involved in hydrogen bond or heme coordination, and selected relevant residues are C-colored white. In both cases, the protein backbone is depicted as ribbons, the dashed lines are drawn between the atoms likely involved in HB or heme coordinations, and selected relevant residues are C-colored white.

Inhibition data in Table 2 indicated that lead compound **1**, with an IC_{50} on CYP19 of $0.150 \mu M$, is a strong inhibitor of both CYP11B1 and CYP11B2 enzymes with IC_{50} values of 0.072 and $0.289 \mu M$, respectively. However, as compared to the well-known ARI fadrozole ($IC_{50} = 0.052 \mu M$ on CYP19), which exhibited IC_{50} values of $0.01 \mu M$ for CYP11B1 and $0.001 \mu M$ for CYP11B2, the CYP19 over CYP11B2 selectivity of **1** was improved nearly 100-fold. Compound **24**, the most potent CYP19 inhibitor of the whole series, showed IC_{50} values of 0.933 and $2.19 \mu M$ for CYP11B1 and CYP11B2, respectively, with an ameliorated selectivity profile as compared to fadrozole. These data might be indicative of less adverse effects potentially arising from the inhibition of the aldosterone biosynthesis.⁶⁰ As a consequence, inhibitors of the 7-aryloxy series appeared safer and more suitable for further preclinical tests as compared to the 7-benzyloxy congeners.

CONCLUSION

In summary, a number of new coumarin imidazolyl derivatives described in this paper proved to be remarkably potent ARIs with a high selectivity over CYP17. CYP11B1 and CYP11B2 inhibition data of lead compounds **1** and **24** suggested that 7-aryloxy derivatives may be safer and more suitable for further development than the 7-benzyloxy congeners.

In comparison with already reported ARIs of similar potency, coumarin derivatives present several advantages, such as a facile and straightforward synthesis and a likely favorable ADMET and toxicological profile as the coumarin scaffold is present in many natural and dietary products⁶¹ and in some drugs as well.⁶² However, some suitably functionalized coumarins may constitute good substrates/inhibitors for some P450 metabolic enzymes.^{63,64} The SAFIR that recently emerged also at this level⁶⁵ may help the design of new compounds with the desired P450 potency, selectivity, and ADMET properties. Simple coumarin chemistry may facilitate the attainment of such important goals since it may allow the introduction of a variety

of properly chosen substituents all around the coumarin ring. Thus, an easy variation of the local and global physicochemical properties of the selected molecules may be possible.

Docking simulations of a selected number of coumarin derivatives allowed the identification of the most important interactions underlying the inhibitor binding and suggested the positions of the coumarin ring suitable for further structural modifications. This molecular mapping might be used to guide the design of new, original inhibitors even based on molecular scaffolds different from coumarin.

EXPERIMENTAL SECTION

Chemistry. High analytical grade chemicals and solvents were from commercial suppliers. When necessary, solvents were dried by standard techniques and distilled. After extraction from aqueous layers, the organic solvents were dried over anhydrous magnesium or sodium sulfate. Thin-layer chromatography (TLC) was performed on aluminum sheets precoated with silica gel 60 F254 (0.2 mm) type (E. Merck). Chromatographic spots were visualized by UV light or Hanessian reagent.⁶⁶ Purification of crude compounds was carried out by flash column chromatography on silica gel 60 (Kieselgel 0.040–0.063 mm, E. Merck) or by crystallization. Melting points (uncorrected) for fully purified products (see below) were determined in a glass capillary tube on a Stuart Scientific electrothermal apparatus SMP3. ¹H NMR spectra were recorded in CDCl₃ (unless otherwise indicated) at 300 MHz on a Varian Mercury 300 instrument. All of the detected signals were in accordance with the proposed structures. Chemical shifts (δ scale) are reported in parts per million (ppm) relative to the central peak of the solvent. Coupling constant (*J* values) are given in Hertz (Hz). Spin multiplicities are given as: s (singlet), s br (broad singlet), d (doublet), dd (double doublet), t (triplet), q (quadruplet), or m (multiplet). ESI-MS was performed with an electrospray interface ion trap mass spectrometer (1100 series LC/MSD Trap System Agilent, Palo Alto, Ca). The purity of all of the intermediates, checked by ¹H NMR and HPLC, was always better than 90%. The purity of all tested final products,

determined by analytical HPLC, was always greater than 95%. Reverse phase HPLC analyses were performed on a system equipped with automatic injector and a Waters Breeze 1525 high performance liquid chromatography (HPLC) pump coupled with a Waters 2489 UV Detector (Waters Corp., Milford, MA) using a Waters XTerra RP 5 μm C8 column (150 mm \times 3.0 mm i. d.). The UV detection was measured at 254 and 280 nm. Each tested compound was analyzed by elution with two different mobile phase systems: In system 1, compounds were eluted using a 80/20 methanol/water mixture at a flow rate of 0.5 mL/min; in system 2, compounds were eluted using a 65/35 acetonitrile/water mixture at a flow rate of 0.5 mL/min. The synthesis of compounds **1**, **14**, **27**, and **33** have been described in a previous paper.³⁰

General Procedure for the Preparation of 7-Benzyloxy-4-(chloromethyl)-2H-chromen-2-one Derivatives 2a–13a. To a solution of 4-(chloromethyl)-7-hydroxycoumarin (0.32 g, 1.5 mmol) in EtOH (15 mL), K_2CO_3 (0.62 g, 4.5 mmol) and the appropriate benzyl bromide (4.5 mmol) were added. The reaction was stirred at reflux for 3 h. After the solution was cooled, K_2CO_3 was filtered off, and the solution was evaporated to dryness. The oily residue was treated with ether obtaining a precipitate that was filtered and used without further purification.

4-(Chloromethyl)-7-[(3-methylbenzyl)oxy]-2H-chromen-2-one (**2a**). Yield, 57%. $^1\text{H NMR}$ δ : 7.56 (d, J = 8.8 Hz, 1H), 7.29–7.15 (m, 4H), 6.98–6.91 (m, 2H), 6.40 (s, 1H), 5.10 (s, 2H), 4.62 (s, 2H), 2.38 (s, 3H).

4-(Chloromethyl)-7-[(3-fluorobenzyl)oxy]-2H-chromen-2-one (**3a**). Yield, 55%. $^1\text{H NMR}$ δ : 7.58 (d, J = 8.8 Hz, 1H), 7.41–7.34 (m, 1H), 7.25–7.13 (m, 2H), 7.07–7.01 (m, 1H), 6.97 (dd, J_1 = 2.5 Hz, J_2 = 8.8 Hz, 1H), 6.89 (d, J = 2.5 Hz, 1H), 6.41 (s, 1H), 5.13 (s, 2H), 4.62 (s, 2H).

7-[(3-Chlorobenzyl)oxy]-4-(chloromethyl)-2H-chromen-2-one (**4a**). Yield, 52%. $^1\text{H NMR}$ δ : 7.64 (d, J = 8.8 Hz, 1H), 7.58–7.55 (m, 1H), 7.43–7.26 (m, 3H), 7.00–6.89 (m, 2H), 6.37 (s, 1H), 5.12 (s, 2H), 4.62 (s, 2H).

4-(Chloromethyl)-7-[(3-(trifluoromethyl)benzyl)oxy]-2H-chromen-2-one (**5a**). Yield, 54%. $^1\text{H NMR}$ δ : 7.43–7.26 (m, 5H), 7.04–6.90 (m, 2H), 6.42 (s, 1H), 5.18 (s, 2H), 4.63 (s, 2H).

4-(Chloromethyl)-7-[(3-(trifluoromethoxy)benzyl)oxy]-2H-chromen-2-one (**6a**). Yield, 51%. $^1\text{H NMR}$ δ : 7.59 (d, J = 8.9 Hz, 1H), 7.49–7.18 (m, 4H), 6.97 (dd, J_1 = 2.6 Hz, J_2 = 8.9 Hz, 1H), 6.91 (d, J = 2.6 Hz, 1H), 6.41 (s, 1H), 5.14 (s, 2H), 4.63 (s, 2H).

4-(Chloromethyl)-7-[(3-nitrobenzyl)oxy]-2H-chromen-2-one (**7a**). Yield, 59%. $^1\text{H NMR}$ δ : 8.33 (s, 1H), 8.21 (d, J = 8.8 Hz, 1H), 7.78 (d, J = 7.7 Hz, 1H), 7.63–7.58 (m, 2H), 7.02–6.91 (m, 2H), 6.43 (s, 1H), 5.23 (s, 2H), 4.63 (s, 2H).

4-(Chloromethyl)-7-[(4-fluorobenzyl)oxy]-2H-chromen-2-one (**8a**). Yield, 58%. $^1\text{H NMR}$ δ : 7.63 (d, J = 8.8 Hz, 1H), 7.42–7.39 (m, 2H), 7.13–7.07 (m, 2H), 6.97–6.90 (m, 2H), 6.41 (s, 1H), 5.10 (s, 2H), 4.62 (s, 2H).

[(4-Chlorobenzyl)oxy]-4-(chloromethyl)-2H-chromen-2-one (**9a**). Yield, 52%. $^1\text{H NMR}$ δ : 7.57 (d, J = 9.0 Hz, 1H), 7.33–7.29 (m, 4H), 6.91–6.87 (m, 2H), 6.41 (s, 1H), 5.10 (s, 2H), 4.55 (s, 2H).

4-(Chloromethyl)-7-[(4-methoxybenzyl)oxy]-2H-chromen-2-one (**10a**). Yield, 35%. $^1\text{H NMR}$ δ : 7.59 (d, J = 8.8 Hz, 1H), 7.47 (d, J = 8.5 Hz, 2H), 7.26–7.24 (m, 4H), 6.40 (s, 1H), 5.06 (s, 2H), 4.55 (s, 2H), 3.82 (s, 3H).

4-(Chloromethyl)-7-[(4-(trifluoromethoxy)benzyl)oxy]-2H-chromen-2-one (**11a**). Yield, 54%. $^1\text{H NMR}$ δ : 7.56 (d, J = 8.8 Hz, 1H), 7.36 (d, J = 8.5 Hz, 2H), 6.97 (d, J = 8.5 Hz, 2H), 6.96 (dd, J_1 = 2.4 Hz, J_2 = 8.8 Hz, 1H), 6.91 (d, J = 2.4 Hz, 1H), 6.41 (s, 1H), 5.13 (s, 2H), 4.63 (s, 2H).

4-(Chloromethyl)-7-[(3,5-difluorobenzyl)oxy]-2H-chromen-2-one (**12a**). Yield, 56%. $^1\text{H NMR}$ δ : 7.59 (d, J = 8.9 Hz, 1H), 6.99–6.95 (m, 3H), 6.87–6.68 (m, 2H), 6.37 (s, 1H), 5.27 (s, 2H), 5.10 (s, 2H).

4-(Chloromethyl)-7-[(3,4-difluorobenzyl)oxy]-2H-chromen-2-one (**13a**). Yield, 55%. $^1\text{H NMR}$ δ : 7.50 (d, J = 8.8 Hz, 1H), 7.19–7.15

(m, 3H), 6.97–6.93 (m, 1H), 6.89–6.88 (m, 1H), 6.42 (s, 1H), 5.08 (s, 2H), 4.62 (s, 2H).

General Procedure for the Preparation of 7-Aryloxy-4-(chloromethyl)-2H-chromen-2-one Derivatives 15a–24a⁴¹. 4-(Chloromethyl)-7-hydroxycoumarin (0.21 g, 1.0 mmol), $\text{Cu}(\text{OAc})_2$ (0.18 g, 1.0 mmol), arylboronic acid (3.0 mmol), and powdered 4 Å molecular sieves were suspended in 10 mL of CH_2Cl_2 , and triethylamine (0.70 mL, 5.0 mmol) was added. The reaction mixture was stirred under ambient atmosphere for 18 h at room temperature. The mixture was filtered over Celite, and the organic filtrate was evaporated to dryness and purified by flash chromatography using a mixture of CH_2Cl_2 /petroleum ether, 8/2 (v/v), as the eluent.

4-(Chloromethyl)-7-(3-fluorophenoxy)-2H-chromen-2-one (**15a**). The product was used for the following reaction without purification. The presence of the desired compound was certified by ESI-MS m/z 305 $[\text{M} + \text{H}]^+$.

4-(Chloromethyl)-7-(3-chlorophenoxy)-2H-chromen-2-one (**16a**). Yield, 30%. $^1\text{H NMR}$ δ : 7.64 (d, J = 8.8 Hz, 1H), 7.35–7.20 (m, 3H), 7.09 (s, 1H), 7.01–6.92 (m, 2H), 6.47 (s, 1H), 4.63 (s, 2H).

4-(Chloromethyl)-7-(3-methoxyphenoxy)-2H-chromen-2-one (**17a**). Yield, 41%. $^1\text{H NMR}$ δ : 7.61 (d, J = 8.8 Hz, 1H), 7.64–7.42 (m, 3H), 7.00–6.80 (m, 3H), 6.44 (s, 1H), 4.65 (s, 2H), 3.81 (s, 3H).

4-(Chloromethyl)-7-(4-methylphenoxy)-2H-chromen-2-one (**18a**). Yield, 44%. $^1\text{H NMR}$ δ : 7.58 (d, J = 8.8 Hz, 1H), 7.22 (d, J = 8.8 Hz, 2H), 6.99–6.93 (m, 3H), 6.84 (d, J = 2.5 Hz, 1H), 6.42 (s, 1H), 4.62 (s, 2H), 2.38 (s, 3H).

4-(Chloromethyl)-7-(4-chlorophenoxy)-2H-chromen-2-one (**19a**). Yield, 42%. $^1\text{H NMR}$ δ : 7.62 (d, J = 8.8 Hz, 1H), 7.38 (d, J = 9.0 Hz, 2H), 7.03 (d, J = 9.0 Hz, 2H), 6.91–6.89 (m, 2H), 6.46 (s, 1H), 5.28 (s, 2H).

4-[[4-(Chloromethyl)-2-oxo-2H-chromen-7-yl]oxy]benzotrile (**20a**). Yield, 49%. $^1\text{H NMR}$ δ : 7.68–7.72 (m, 3H), 7.13 (d, J = 9.0 Hz, 2H), 7.04–7.01 (m, 2H), 6.51 (s, 1H), 4.64 (s, 2H).

7-(4-Acetylphenoxy)-4-(chloromethyl)-2H-chromen-2-one (**21a**). Yield, 44%. $^1\text{H NMR}$ δ : 8.01 (d, J = 8.5 Hz, 2H), 7.64 (d, J = 8.8 Hz, 1H), 7.12 (d, J = 8.5 Hz, 2H), 7.02–7.03 (m, 2H), 6.49 (s, 1H), 4.64 (s, 2H), 2.61 (s, 3H).

4-(Chloromethyl)-7-[4-(dimethylamino)phenoxy]-2H-chromen-2-one (**22a**). Yield, 48%. $^1\text{H NMR}$ δ : 7.54 (d, J = 9.0 Hz, 1H), 6.99–6.90 (m, 3H), 6.79–6.68 (m, 3H), 6.39 (s, 1H), 4.60 (s, 2H), 2.96 (s, 6H).

4-(Chloromethyl)-7-(3,5-difluorophenoxy)-2H-chromen-2-one (**23a**). The residue was used for the following reaction without purification. The presence of the desired compound was certified by ESI-MS m/z 345 $[\text{M} + \text{Na}]^+$.

4-(Chloromethyl)-7-(3,4-difluorophenoxy)-2H-chromen-2-one (**24a**). Yield, 43%. $^1\text{H NMR}$ δ : 7.64 (d, J = 8.8 Hz, 1H), 7.21–7.23 (m, 1H), 6.93–6.97 (m, 4H), 6.47 (s, 1H), 4.63 (s, 2H).

General Procedure for the Preparation of (1H-Imidazol-1-ylmethyl)coumarin Derivatives 2–13, 15–24, and 26. To a solution of imidazole (0.081 g, 1.2 mmol) in THF (2 mL), K_2CO_3 (0.17 g, 1.2 mmol) and the suitable (chloromethyl)coumarin derivative (0.41 mmol) were added. The reaction mixture was refluxed for 5–7 h. After it was cooled, the inorganic residue was filtered off, and the solution was evaporated to dryness. The crude residue was recrystallized from ethanol.

4-(1H-Imidazol-1-ylmethyl)-7-[(3-methylbenzyl)oxy]-2H-chromen-2-one (**2**). Yield, 69%; mp 118–120 °C. $^1\text{H NMR}$ δ : 7.58 (d, J = 8.8 Hz, 1H), 7.31–7.15 (m, 7H), 6.98–6.91 (m, 2H), 5.86 (s, 1H), 5.72 (s, 2H), 5.09 (s, 2H), 2.37 (s, 3H). ESI-MS: m/z 347 $[\text{M} + \text{H}]^+$.

7-[(3-Fluorobenzyl)oxy]-4-(1H-imidazol-1-ylmethyl)-2H-chromen-2-one (**3**). Yield, 65%; mp 175–178 °C. $^1\text{H NMR}$ δ : 8.50 (s, 1H), 7.50 (d, J = 8.8 Hz, 1H), 7.38–7.27 (m, 3H), 7.18–6.90 (m, 5H), 5.76 (s, 1H), 5.49 (s, 2H), 5.12 (s, 2H). ESI-MS: m/z 351 $[\text{M} + \text{H}]^+$.

7-[(3-Chlorobenzyl)oxy]-4-(1H-imidazol-1-ylmethyl)-2H-chromen-2-one (**4**). Yield, 62%; mp 127–129 °C. $^1\text{H NMR}$ δ : 8.83 (s, 1H), 7.54

(d, $J = 8.8$ Hz, 1H), 7.42 (s, 1H), 7.35–7.29 (m, 4H), 7.06 (s, 1H), 6.95 (dd, $J_1 = 2.5$ Hz, $J_2 = 8.8$ Hz, 1H), 6.91 (d, $J = 2.5$ Hz, 1H), 5.81 (s, 1H), 5.57 (s, 2H), 5.11 (s, 2H). ESI-MS: m/z 367 [M + H]⁺.

4-(1H-Imidazol-1-ylmethyl)-7-[(3-(trifluoromethyl)benzyl)oxy]-2H-chromen-2-one (**5**). Yield, 52%; mp 136–138 °C. ¹H NMR δ : 8.80 (s, br, 1H), 7.70 (s, 1H), 7.63–7.61 (m, 2H), 7.56–7.51 (m, 3H), 6.99–6.92 (m, 3H), 5.79 (s, 1H), 5.51 (s, 2H), 5.18 (s, 2H). ESI-MS: m/z 401 [M + H]⁺.

4-(1H-Imidazol-1-ylmethyl)-7-[(3-(trifluoromethoxy)benzyl)oxy]-2H-chromen-2-one (**6**). Yield, 57%; mp 102–104 °C. ¹H NMR δ : 8.01 (s, 1H), 7.60 (s, 1H), 7.47–7.44 (m, 2H), 7.42–7.37 (m, 1H), 7.29 (s, 1H), 7.22–7.17 (m, 2H), 6.98–6.92 (m, 2H), 5.72 (s, 1H), 5.29 (s, 2H), 5.15 (s, 2H). ESI-MS: m/z 417 [M + H]⁺.

4-(1H-Imidazol-1-ylmethyl)-7-[(3-nitrobenzyl)oxy]-2H-chromen-2-one (**7**). Yield, 62%; mp 218–221 °C. ¹H NMR δ : 8.29 (s, 1H), 8.14–8.20 (m, 2H), 7.75 (d, $J = 8.8$ Hz, 1H), 7.49–7.61 (m, 2H), 7.20 (s, 1H), 6.91–7.04 (m, 3H), 5.73 (s, 1H), 5.42 (s, 2H), 5.21 (s, 2H). ESI-MS: m/z 378 [M + H]⁺.

7-[(4-Fluorobenzyl)oxy]-4-(1H-imidazol-1-ylmethyl)-2H-chromen-2-one (**8**). Yield, 66%; mp 138–140 °C. ¹H NMR δ : 9.66 (s, 1H), 7.64 (d, $J = 8.8$ Hz, 1H), 7.38–7.41 (m, 3H), 7.17–7.25 (m, 3H), 7.09 (m, 2H), 5.85 (s, 1H), 5.81 (s, 2H), 5.09 (s, 2H). ESI-MS: m/z 351 [M + H]⁺.

7-[(4-Chlorobenzyl)oxy]-4-(1H-imidazol-1-ylmethyl)-2H-chromen-2-one (**9**). Yield, 20%; mp >220 °C. ¹H NMR δ : 7.58 (s, 1H), 7.42–7.36 (m, 5H), 7.18 (s, 1H), 6.96–6.92 (m, 3H), 5.73 (s, 1H), 5.27 (s, 2H), 5.10 (s, 2H). ESI-MS: m/z 365 [M – H][–].

4-(1H-Imidazol-1-ylmethyl)-7-[(4-methoxybenzyl)oxy]-2H-chromen-2-one (**10**). Yield, 20%; mp 209–211 °C. ¹H NMR δ : 7.58 (s, 1H), 7.28–7.34 (m, 4H), 7.18 (s, 1H), 6.96–6.92 (m, 4H), 5.72 (s, 1H), 5.26 (s, 2H), 5.06 (s, 2H), 3.82 (s, 3H). ESI-MS: m/z 361 [M – H][–].

4-(1H-Imidazol-1-ylmethyl)-7-[(4-trifluoromethoxybenzyl)oxy]-2H-chromen-2-one (**11**). Yield, 51%; mp 102–104 °C. ¹H NMR δ : 7.67 (s, 1H), 7.48–7.41 (m, 2H), 7.26–7.20 (m, 4H), 7.17 (s, 1H), 6.96–6.92 (m, 2H), 5.75 (s, 1H), 5.29 (s, 2H), 5.13 (s, 2H). ESI-MS: m/z 415 [M – H][–].

7-[(3,5-Difluorobenzyl)oxy]-4-(1H-imidazol-1-ylmethyl)-2H-chromen-2-one (**12**). Yield, 22%; mp 170–172 °C. ¹H NMR δ : 7.57 (s, 1H), 7.43 (d, $J = 9.0$ Hz, 1H), 7.20 (s, 1H), 6.95–6.80 (m, 5H), 6.81–6.79 (m, 1H), 5.78 (s, 1H), 5.20 (s, 2H), 5.08 (s, 2H). ESI-MS: m/z 367 [M – H][–].

7-[(3,4-Difluorobenzyl)oxy]-4-(1H-imidazol-1-ylmethyl)-2H-chromen-2-one (**13**). Yield, 63%; mp 91–93 °C. ¹H NMR δ : 9.61 (s, 1H), 7.60 (d, $J = 8.8$ Hz, 1H), 7.25–7.15 (m, 4H), 7.17–6.89 (m, 3H), 5.74 (s, 1H), 5.18 (s, 2H), 5.08 (s, 2H). ESI-MS: m/z 369 [M + H]⁺.

7-(3-Fluorophenoxy)-4-(1H-imidazol-1-ylmethyl)-2H-chromen-2-one (**15**). Yield, 25%; mp 108–110 °C. ¹H NMR δ : 8.08 (s, 1H), 7.45 (d, $J = 9.0$ Hz, 1H), 7.40–7.30 (m, 2H), 7.00–6.80 (m, 4H), 5.80 (s, 1H), 5.40 (s, 2H), two imidazole protons were not detected. ESI-MS: m/z 335 [M – H][–].

7-(3-Chlorophenoxy)-4-(1H-imidazol-1-ylmethyl)-2H-chromen-2-one (**16**). Yield, 62%; mp 137 °C (dec). ¹H NMR δ : 7.99 (s, 1H), 7.51 (d, $J = 8.8$ Hz, 1H), 7.32–7.35 (m, 4H), 7.09–6.92 (m, 4H), 5.81 (s, 1H), 5.39 (s, 2H). ESI-MS: m/z 353 [M + H]⁺.

4-(1H-Imidazol-1-ylmethyl)-7-(3-methoxyphenoxy)-2H-chromen-2-one (**17**). Yield, 67%; amorphous solid. ¹H NMR δ : 8.85 (s, 1H), 7.58 (d, $J = 8.8$ Hz, 1H), 7.35–6.65 (m, 8H), 5.84 (s, 1H), 5.70 (s, 2H), 3.81 (s, 3H). ESI-MS: m/z 349 [M + H]⁺.

4-(1H-Imidazol-1-ylmethyl)-7-(4-methylphenoxy)-2H-chromen-2-one (**18**). Yield, 32%; mp 106–108 °C. ¹H NMR δ : 9.96 (s, 1H), 7.65 (d, $J = 8.5$ Hz, 1H), 7.41 (s, 1H), 7.23 (d, $J = 8.4$ Hz, 2H), 7.15 (s, 1H), 6.98–6.94 (m, 3H), 6.84 (d, $J = 2.5$ Hz, 1H), 5.94 (s, 1H), 5.83 (s, 2H), 2.38 (s, 3H). ESI-MS: m/z 333 [M + H]⁺.

7-(4-Chlorophenoxy)-4-(1H-imidazol-1-ylmethyl)-2H-chromen-2-one (**19**). Yield, 65%; mp >250 °C. ¹H NMR δ : 8.03 (s, 1H), 7.51

(d, $J = 8.8$ Hz, 1H), 7.38 (d, $J = 8.8$ Hz, 2H), 7.03 (d, $J = 8.8$ Hz, 2H), 6.95–6.85 (m, 4H), 5.80 (s, 1H), 5.42 (s, 2H). ESI-MS: m/z 353 [M + H]⁺.

4-[(4-(1H-Imidazol-1-ylmethyl)-2-oxo-2H-chromen-7-yl)oxy]benzotrile (**20**). Yield, 61%; mp 145–147 °C. ¹H NMR δ : 8.71 (s, 1H), 7.69–7.66 (m, 3H), 7.15–7.13 (m, 3H), 6.99–6.98 (m, 3H), 5.85 (s, 1H), 5.58 (s, 2H). ESI-MS: m/z 344 [M + H]⁺.

7-(4-Acetylphenoxy)-4-(1H-imidazol-1-ylmethyl)-2H-chromen-2-one (**21**). Yield, 62%; mp 157–160 °C. ¹H NMR δ : 8.04–8.00 (m, 4H), 7.87 (d, $J = 8.5$ Hz, 1H), 7.54 (d, $J = 9.0$ Hz, 2H), 7.12 (dd, $J_1 = 2.6$ Hz, $J_2 = 8.8$ Hz, 1H), 7.02–6.99 (m, 1H), 6.91 (d, $J = 2.6$ Hz, 1H), 5.84 (s, 1H), 5.41 (s, 2H), 2.61 (s, 3H). ESI-MS: m/z 361 [M + H]⁺.

7-[4-(Dimethylamino)phenoxy]-4-(1H-imidazol-1-ylmethyl)-2H-chromen-2-one (**22**). Yield, 67%; oily product. ¹H NMR δ : 7.60 (s, 1H), 7.39 (d, $J = 8.8$ Hz, 1H), 7.17 (s, 1H), 6.98–6.95 (m, 3H), 6.76–6.73 (m, 4H), 5.70 (s, 1H), 5.27 (s, 2H), 2.96 (s, 6H). ESI-MS: m/z 362 [M + H]⁺.

7-(3,5-Difluorophenoxy)-4-(1H-imidazol-1-ylmethyl)-2H-chromen-2-one (**23**). Yield, 29%; mp 119–120 °C. ¹H NMR δ : 7.68 (s, 1H), 7.51 (d, $J = 9.6$ Hz, 1H), 7.21 (s, 1H), 7.10–6.90 (m, 3H), 6.80–6.50 (m, 3H), 5.80 (s, 1H), 5.32 (s, 2H). ESI-MS: m/z 353 [M – H][–].

7-(3,4-Difluorophenoxy)-4-(1H-imidazol-1-ylmethyl)-2H-chromen-2-one (**24**). Yield, 66%; mp 80–83 °C. ¹H NMR δ : 7.70 (s, 1H), 7.59 (s, 1H), 7.48 (d, $J = 8.8$ Hz, 1H), 7.26–7.17 (m, 3H), 6.88–6.97 (m, 3H), 5.76 (s, 1H), 5.30 (s, 2H). ESI-MS: m/z 355 [M + H]⁺.

7-Hydroxy-4-(1H-imidazol-1-ylmethyl)-2H-chromen-2-one (**26**). Yield, 74%; mp >250 °C. ¹H NMR (DMSO-*d*₆) δ : 10.55 (s, 1H), 7.83 (s, 1H), 7.87–7.76 (m, 1H), 7.26 (s, 1H), 7.01 (s, 1H), 6.83–6.73 (m, 2H), 5.51 (s, 2H), 5.38 (s, 1H). ESI-MS: m/z 241 [M – H][–].

4-Chloromethyl-2-oxo-2H-chromen-7-yl-carbamic Acid Ethyl Ester (**25b**). Ethyl chloroacetate (1.3 g, 7.8 mmol) and **25a**⁴² (1.0 g, 5.5 mmol) were suspended in 13 mL of 70% H₂SO₄ and were stirred at room temperature for 4 h. The mixture was poured in 50 mL of ice water, giving a white precipitate that was crystallized from absolute EtOH. Yield, 83%. ¹H NMR δ : 8.62 (s, 1H), 7.54–7.40 (m, 3H), 6.37 (s, 1H), 4.59 (s, 2H), 4.17 (q, $J = 7.4$ Hz, 2H), 1.25 (t, $J = 7.4$ Hz, 3H).

7-Amino-4-chloromethyl-2H-chromen-2-one (**25c**). Derivative **25b** (0.43 g, 1.5 mmol) was dissolved in a solution of 20 mL of concentrated H₂SO₄ and 20 mL of glacial acetic acid, and the mixture was heated at reflux for 4 h. After it was cooled, the mixture was poured in 400 mL of ice water. At 0 °C, 50% NaOH was added until the solution resulted slightly alkaline. The obtained precipitate was filtered and washed with ice water (3 × 50 mL). Yield, 62%. ¹H NMR δ : 7.45 (d, $J = 8.8$ Hz, 1H), 6.58 (dd, $J_1 = 2.2$ Hz, $J_2 = 8.8$ Hz, 1H), 6.41 (d, $J = 2.2$ Hz, 1H), 6.22 (s, 2H), 6.16 (s, 1H), 4.85 (s, 2H).

4-Chloromethyl-7-phenylamino-2H-chromen-2-one (**25d**). Compound **25c** (0.11 g, 0.50 mmol), benzenboronic acid (0.12 g, 1.0 mmol), Cu(OAc)₂ (0.090 g, 0.50 mmol), and triethylamine (0.14 mL, 1.0 mmol) were dissolved in 10 mL of CH₂Cl₂, and the mixture was stirred at room temperature for 72 h. The solvent was evaporated to dryness, and the product was purified by flash chromatography by using CH₂Cl₂ as the eluent. Yield, 35%. ¹H NMR δ : 8.98 (s, 1H), 7.64 (d, $J = 8.8$ Hz, 1H), 7.36–7.31 (m, 2H), 7.22–7.19 (m, 2H), 7.02–6.99 (m, 2H), 6.88 (s, 1H), 6.32 (s, 1H), 4.92 (s, 2H).

7-Anilino-4-(1H-imidazol-1-ylmethyl)-2H-chromen-2-one (**25**). To a solution of imidazole (0.082 g, 1.2 mmol), in THF (2.0 mL), K₂CO₃ (0.33 g, 2.4 mmol), and **25d** (0.12 g, 0.41 mmol) were added. The mixture was heated at reflux for 7 h. After the mixture was cooled, the inorganic residue was filtered off, and the organic solution was dried under vacuum. The crude product was purified by flash chromatography using a mixture of CHCl₃/MeOH, 9:1 (v/v) as the eluent. Yield, 60%; oily residue. ¹H NMR δ : 8.99 (s, 1H), 7.84 (s, 1H), 7.66 (d, $J = 8.8$ Hz, 1H), 7.37–7.32 (m, 3H), 7.23–7.10 (m, 2H), 7.02–6.96 (m, 3H), 6.88 (d, $J = 2.2$ Hz, 1H), 5.48 (s, 1H), 5.31 (s, 2H). ESI-MS: m/z 318 [M + H]⁺.

4-Benzyl-7-methoxy-2H-chromen-2-one (**28b**). Derivative **28a**⁴⁶ (11 mmol, 2.8 g) was dissolved in DMF (45 mL), and the solution was cooled to 0 °C. NaH (0.60 g, 25 mmol) was slowly added to the solution followed by 20 min of stirring. CH₃I (1.6 mL, 25 mmol) was then added to the reaction mixture that slowly reached room temperature. After 1 h, the mixture was poured onto ice and extracted with EtOAc (3 × 10 mL). The organic layer was extracted with a 2 N solution of NaOH (3 × 5 mL) and water (3 × 5 mL), dried over Na₂SO₄, and then concentrated under vacuum to give the desired derivative. Yield, 43%. ¹H NMR δ: 7.47 (d, *J* = 8.8 Hz, 1H), 7.35–7.16 (m, 5H), 6.84–6.75 (m, 2H), 6.00 (s, 1H), 4.05 (s, 2H), 3.85 (s, 3H). ESI-MS: *m/z* 251 [M – H][–].

4-[Bromo(phenyl)methyl]-7-methoxy-2H-chromen-2-one (**28c**). To the solution of **28b** (0.18 g, 0.69 mmol) in CCl₄ (2.5 mL) were added *N*-bromosuccinimide (0.15 g, 0.83 mmol) and a catalytic amount of benzoyl peroxide. The reaction mixture was refluxed until the disappearance of the starting material (about 2 h). The succinimide was rapidly filtered off, and the desired solid product was recovered after cooling and used in the next step without further purification. Yield, 38%. ¹H NMR δ: 7.53 (d, *J* = 8.8 Hz, 1H), 7.46–7.34 (m, 5H), 6.84–6.80 (m, 2H), 6.48 (s, 1H), 6.33 (s, 1H), 3.85 (s, 3H).

4-[1H-Imidazol-1-yl(phenyl)methyl]-7-methoxy-2H-chromen-2-one (**28**). To a solution of imidazole (0.082 g, 1.2 mmol) in THF (2 mL) were added K₂CO₃ (0.17 g, 1.2 mmol) and **28c** (0.15 g, 0.41 mmol). The reaction mixture was refluxed for 5–7 h. After the mixture was cooled, the inorganic residue was filtered off, and the solution was evaporated to dryness. Yield, 45%; amorphous solid. ¹H NMR δ: 8.23 (s br, 1H), 7.58 (d, *J* = 8.8 Hz, 1H), 7.46–7.18 (m, 7H), 6.89–6.85 (m, 2H), 5.64 (s, 1H), 3.85 (s, 3H), one imidazole proton was not detected. ESI-MS: *m/z* 333 [M + H]⁺. The synthesis of derivatives **31a** and **32a** was done as described for compound **29a**.⁴⁵

4-(4-Chlorophenyl)-3-oxobutanoic Acid Ethyl Ester (**31a**). Yield, 50%. ¹H NMR δ: 7.29 (d, *J* = 9.0 Hz, 2H), 7.24 (d, *J* = 9.0 Hz, 2H), 4.16 (q, *J* = 7.2 Hz, 2H), 3.80 (s, 2H), 3.44 (s, 2H), 1.25 (t, *J* = 7.2 Hz, 3H).

4-(4-Cyanophenyl)-3-oxobutanoic Acid Ethyl Ester (**32a**). Yield, 52%. ¹H NMR δ: 7.61 (d, *J* = 8.4 Hz, 2H), 7.30 (d, *J* = 8.4 Hz, 2H), 4.17 (q, *J* = 7.2 Hz, 2H), 3.92 (s, 2H), 3.48 (s, 2H), 1.25 (t, *J* = 7.2 Hz, 3H).

General Procedure for the Synthesis of 7-Phenoxy-4-arylmethyl-2H-chromen-2-ones 29b, 31b, and 32b. The appropriate ethyl phenylacetate (6.4 mmol) was charged in a flask, and 3-phenoxyphenol (1.0 g, 5.4 mmol) was added. The mixture was stirred at 120 °C, and 2 drops of concentrated H₂SO₄ were added. After 30 min, the mixture was allowed to reach room temperature, and later, it was poured in ice water (100 mL). The product was extracted with CHCl₃, and the organic layer was dried over Na₂SO₄ and evaporated to dryness to give an oil that was purified by flash chromatography using a mixture of CHCl₃/*n*-hexanes, 7:3 (v/v), as the eluent.

4-Benzyl-7-phenoxy-2H-chromen-2-one (**29b**). Yield, 54%. ¹H NMR δ: 7.98 (d, *J* = 8.5 Hz, 1H), 7.71–7.21 (m, 8H), 7.11–7.06 (m, 2H), 6.95–6.78 (m, 2H), 6.03 (s, 1H), 4.07 (s, 2H).

4-(4-Chlorobenzyl)-7-phenoxy-2H-chromen-2-one (**31b**). Yield, 20%. ¹H NMR δ: 7.49 (d, *J* = 9.0 Hz, 1H), 7.42–7.38 (m, 3H), 7.31 (d, *J* = 8.9 Hz, 2H), 7.33–7.30 (m, 2H), 7.15 (d, *J* = 8.9 Hz, 2H), 7.06–7.04 (m, 1H), 6.85–6.82 (m, 1H), 6.01 (s, 1H), 4.04 (s, 2H).

4-(2-Oxo-7-phenoxy-2H-chromen-4-ylmethyl)-benzotrile (**32b**). Yield, 35%. ¹H NMR δ: 7.64 (d, *J* = 8.1 Hz, 2H), 7.50–7.30 (m, 5H), 7.24 (s, 1H), 7.06 (d, 2H, *J* = 8.1 Hz), 6.82 (m, 2H), 6.01 (s, 1H), 4.13 (s, 2H).

General Procedure for the Preparation of 4-[Bromo(aryl)methyl]-7-phenoxy-2H-chromen-2-ones 29c, 31c, and 32c. The chosen coumarin (0.61 mmol) and *N*-bromosuccinimide (0.13 g, 0.73 mmol) were dissolved in 2 mL of CCl₄. The mixture was heated at reflux, and a catalytic amount of dibenzoyl peroxide was added. The mixture was refluxed for 1 h. Succinimide was filtered off, and the

filtrate was evaporated to dryness. The residue was purified by flash chromatography by using CHCl₃ as the eluent.

4-[Bromo(phenyl)methyl]-7-phenoxy-2H-chromen-2-one (**29c**). Yield, 33%. ¹H NMR δ: 8.08 (d, *J* = 7.2 Hz, 1H), 7.83–7.25 (m, 8H), 7.09–7.05 (m, 2H), 6.86–6.83 (m, 2H), 6.43 (s, 1H), 6.33 (s, 1H).

4-[Bromo(4-chlorophenyl)methyl]-7-phenoxy-2H-chromen-2-one (**31c**). Yield, 47%. ¹H NMR δ: 7.50 (d, *J* = 8.7 Hz, 1H), 7.46–7.34 (m, 7H), 7.07 (d, *J* = 7.5 Hz, 2H), 6.87 (m, 2H), 6.50 (s, 1H), 6.29 (s, 1H).

4-[Bromo(2-oxo-7-phenoxy-2H-chromen-4-yl)methyl]benzotrile (**32c**). Yield, 81%. ¹H NMR δ: 8.04 (d, *J* = 8.7 Hz, 2H), 7.82 (d, *J* = 8.7 Hz, 2H), 7.80–7.59 (m, 2H), 7.42–7.35 (m, 2H), 7.15–7.01 (m, 2H), 6.90–6.75 (m, 3H), 6.26 (s, 1H).

General Procedure for the Preparation 4-[1H-Imidazol-1-yl(aryl)methyl]-7-phenoxy-2H-chromen-2-ones 29, 31, and 32. The appropriate bromide (0.085 mmol) was dissolved in 5 mL of dry acetonitrile. Imidazole (0.058 g, 0.85 mmol) was added, and the mixture was refluxed for 5 h. The solvent was evaporated to dryness, and the residue was purified by chromatography using as the eluent a mixture of CHCl₃/MeOH, 9/1 (v/v).

4-[1H-Imidazol-1-yl(phenyl)methyl]-7-phenoxy-2H-chromen-2-one (**29**). Yield, 95%; mp 92–94 °C. ¹H NMR δ: 9.62 (s, 1H), 7.98 (s, 1H), 7.58–7.30 (m, 10H), 7.05–7.01 (m, 3H), 6.90–6.79 (m, 2H), 5.69 (s, 1H). ESI-MS: *m/z* 395 [M + H]⁺.

4-[(4-Chlorophenyl)(1H-imidazol-1-yl)methyl]-7-phenoxy-2H-chromen-2-one (**31**). Yield, 41%; mp 86–88 °C. ¹H NMR δ: 9.88 (s, 1H), 8.24 (s, 1H), 7.44–7.38 (m, 10H), 7.05 (d, *J* = 9.0 Hz, 1H), 6.84 (m, 2H), 5.68 (s, 1H), one imidazole proton was not detected. ESI-MS: *m/z* 451 [M + Na]⁺.

4-[1H-Imidazol-1-yl(2-oxo-7-phenoxy-2H-chromen-4-yl)methyl]benzotrile (**32**). Yield, 69%; amorphous solid. ¹H NMR δ: 9.82 (s, 1H), 8.34 (s, 1H), 7.75 (d, *J* = 9.0 Hz, 2H), 7.61 (d, *J* = 9.0 Hz, 2H), 7.39 (m, 4H), 7.25 (s, 1H), 7.04 (d, *J* = 7.2 Hz, 2H), 6.96 (s, 1H), 6.85 (m, 2H), 5.72 (s, 1H). ESI-MS: *m/z* 420 [M + H]⁺.

Synthesis of 4-Benzyl-7-(3,4-difluorophenoxy)-2H-chromen-2-one (30a). Intermediate **28a** (0.050 g, 0.20 mmol) was suspended in 2 mL of dry CH₂Cl₂. 3,4-F₂-benzeneboronic acid (0.11 g, 0.70 mmol), Cu(OAc)₂ (0.036 g, 0.20 mmol), and triethylamine (0.14 mL, 1.0 mmol) were added. The reaction was stirred at room temperature for 4 h. The mixture was filtered over Celite. The filtrate was evaporated to dryness giving a residue that was purified by flash chromatography by using CHCl₃ as the eluent. Yield, 20%. ¹H NMR δ: 7.59 (d, *J* = 9.1 Hz, 1H), 7.37–7.17 (m, 6H), 6.98–6.78 (m, 4H), 6.07 (s, 1H), 4.08 (s, 2H).

4-[Bromo(phenyl)methyl]-7-(3,4-difluorophenoxy)-2H-chromen-2-one (**30b**). Coumarin **30a** (0.021 g, 0.051 mmol) and NBS (0.011 g, 0.060 mmol) were dissolved in 2 mL of CCl₄. The mixture was heated at reflux, and a catalytic amount of DBP was added. After 4 h, the hot mixture was filtered, and the filtrate was evaporated to dryness. The residue obtained was used without purification for the next reaction.

7-(3,4-Difluorophenoxy)-4-[1H-imidazol-1-yl(phenyl)methyl]-2H-chromen-2-one (**30**). Intermediate **30b** (0.022 g, 0.050 mmol) was dissolved in 2 mL of dry acetonitrile, and imidazole (0.034 g, 0.50 mmol) was added. The mixture was heated at reflux for 6 h. The solvent was evaporated to dryness, and the residue was purified by flash chromatography using as the eluent a mixture of CHCl₃/MeOH, 9:1 (v/v). Yield, 21%; mp 86–88 °C. ¹H NMR δ: 7.96 (s, 1H), 7.72–7.69 (m, 1H), 7.54–7.51 (m, 1H), 7.47–7.44 (m, 2H), 7.31–7.28 (m, 2H), 7.24–7.15 (m, 3H), 7.00 (s, 1H), 6.94–6.87 (m, 2H), 6.84–6.75 (m, 2H), 5.78 (s, 1H). ESI-MS: *m/z* 429 [M – H][–].

3-Benzyl-7-hydroxy-2H-chromen-2-one (**34b**). 3-Benzyl-7-methoxy-2H-chromen-2-one **34a**⁴⁶ (0.27 g, 1.0 mmol) was dissolved in 2 mL of dry CH₂Cl₂, and 1 M BBr₃ in dry CH₂Cl₂ (2.5 mL) was added dropwise at 0 °C. The mixture was allowed to reach room temperature, and after it was stirred for 18 h, it was poured in ice water, stirring vigorously. The obtained precipitate was filtered and used without further purification. Yield, 99%.

^1H NMR δ : 10.42 (s, 1H), 7.68 (s, 1H), 7.43 (d, $J = 8.4$ Hz, 1H), 7.35–7.15 (m, 5H), 6.80–6.65 (m, 2H), 3.72 (s, 2H).

3-Benzyl-7-phenoxy-2H-chromen-2-one (34c). Intermediate **34b** (0.20 g, 0.80 mmol) was suspended in 2 mL of dry CH_2Cl_2 . Benzeneboronic acid (0.98 g, 0.80 mmol), $\text{Cu}(\text{OAc})_2$ (0.15 g, 0.80 mmol), and triethylamine (0.56 mL, 4.0 mmol) were added. The reaction was stirred at room temperature for 1 h. The mixture was filtered over Celite. The filtrate was evaporated to dryness giving a residue that was purified by flash chromatography using a mixture of petroleum ether/ CHCl_3 , 3/7 (v/v), as the eluent. Yield, 29%. ^1H NMR δ : 7.42–7.18 (m, 10H), 7.12–7.03 (m, 2H), 6.90–6.81 (m, 2H), 3.85 (s, 2H).

3-[Bromo(phenyl)methyl]-7-phenoxy-2H-chromen-2-one (34d). Coumarin **34c** (0.072 g, 0.22 mmol) and *N*-bromosuccinimide (0.047 g, 0.26 mmol) were dissolved in 4 mL of CCl_4 . The mixture was heated at reflux, and a catalytic amount of DBP was added. After 4 h, the hot mixture was filtered, and the filtrate was evaporated to dryness. The residue was purified by flash chromatography by using CHCl_3 as the eluent. Yield, 30%. ^1H NMR δ : 7.82 (s, 1H), 7.45–7.18 (m, 9H), 7.10–7.01 (m, 2H), 6.92 (dd, $J_1 = 2.5$ Hz, $J_2 = 8.8$ Hz, 1H), 6.86 (d, $J = 2.5$ Hz, 1H), 5.50 (s, 1H).

3-[1H-Imidazol-1-yl(phenyl)methyl]-7-phenoxy-2H-chromen-2-one (34). Intermediate **34d** (0.074 g, 0.184 mmol) was dissolved in 4 mL of dry acetonitrile, imidazole (0.037 g, 0.55 mmol) was added, and the mixture was refluxed for 6 h. The solvent was evaporated to dryness, and the residue purified by flash chromatography using a mixture of CHCl_3 /MeOH, 9:1 (v/v), as the eluent. Yield, 41%; mp 88–90 °C. ^1H NMR δ : 8.07 (s, 1H), 7.48–7.38 (m, 7H), 7.34 (s, 1H), 7.28 (s, 1H), 7.26–7.24 (m, 2H), 6.91 (dd, $J_1 = 2.5$ Hz, $J_2 = 8.8$ Hz, 1H), 6.85 (d, $J = 2.5$ Hz, 1H), 6.77 (s, 1H). ESI-MS: m/z 417 [$M + \text{Na}$] $^+$.

Biological Assays. *Cellular Assays for Testing CYP19 and CYP17 Inhibition.* As a source of the enzymes, used were the following microsomal preparations: for CYP19, human placenta,^{14,47} for CYP17, *E. coli*-expressing human CYP17.^{48,49} The CYP19 assay was performed as described using the $^3\text{H}_2\text{O}$ method: [1β - ^3H]androstenedione/androstenedione (0.5 μM)⁴⁷ was used as substrate. The CYP17 assay was performed with nonlabeled progesterone, and an HPLC procedure was employed for the separation of the substrate and androstenedione using UV detection.^{48,67}

Cellular Assays for Testing CYP11B1 and CYP11B2 Inhibition. V79MZ/h11B1 and V79MZ/h11B2 cell lines were cultivated in Dulbecco's modified Eagle's medium supplemented with 5% fetal calf serum, penicillin (100 U/mL), streptomycin (100 $\mu\text{g}/\text{mL}$), glutamine (2 mM), and sodium pyruvate (1 mM) at 37 °C in 5% CO_2 in air.

V79MZ cells expressing human CYP11B1 and human CYP11B2 genes, respectively, were grown on 24-well cell culture plates (8×10^5 cells per well) with 1.9 cm^2 culture area per well in 1 mL of DMEM culture medium until confluence. Before testing, the DMEM culture medium was removed, and 450 μL of fresh DMEM, containing the inhibitor, was added to each well. Every value was determined at least three times. After a preincubation step of 60 min at 37 °C, the reaction was started by the addition of 50 μL of DMEM containing the substrate 11-deoxycorticosterone (containing 0.15 μCi of [$1,2$ - ^3H]-11-deoxycorticosterone, dissolved in ethanol; final concentration, 100 nM). The V79MZ/h11B1 cells were incubated for 25 min, the V79MZ/h11B2 cells were incubated for 50 min. Controls were treated in the same way without inhibitors. The maximum DMSO concentration in each well was 1%. Enzyme reactions were stopped by extracting the supernatant with 500 μL of ethyl acetate. Samples were centrifuged (1000g, 2 min), and the solvent was pipetted into fresh cups. The solvent was evaporated, and the steroids were redissolved in 40 μL of methanol and analyzed by HPLC using radioflow detection.

Molecular Modeling. Docking calculations were performed through an induced fit docking procedure, using the X-ray crystallographic structure of the human AR enzyme, available at the wwPDB³¹ (PDB id 3eqm³⁸). The model was imported in Maestro⁶⁸ and then treated with the available preparation wizard tool using standard settings. After the addition of hydrogen atoms and the manual correction of wrongly assigned bond orders, the final

structure was mildly minimized (rmsd convergence criterion set to 0.30 Å) to eliminate, where present, steric clashes. At first, lead compound **14** was allowed to look for favorable poses within a box centered on the androstenedione (the cognate ligand in the X-ray structure) and spanning 20 Å in each of the three directions so to contain entirely the protein active site. During the run, the van der Waals radii of nonpolar atoms were scaled by a factor of 0.3 both for the protein and for the ligand to induce a permissive allocation of the ligand. Moreover, a metal bond constraint was used to funnel the search protocol toward iron-coordinating poses and hydroxyl groups of amino acid side chains enclosed in the box were allowed to rotate. The main purpose of this step was to provide a reasonable starting complex with which to work. The final model, comprising compound **14** top-ranked pose and the enzyme, was subsequently energy minimized, using MacroModel,⁶⁹ upon one distance (Fe-coordinating N equilibrium distance set to 2.4 Å) and one angle (Fe-coordinating N and noncoordinating N of the imidazole ring equilibrium angle set to 180°) constraints to explicitly account for the iron coordination. The so obtained relaxed complex was then used to dock selected compounds at the active site. The rmsd, calculated over all of the heavy atoms within 5 Å of lead compound **14**, between the so obtained model and the starting structure was as small as 1.2 Å. The docking simulations were performed through the Induced Fit Docking⁷⁰ (IFD) protocol as implemented in the Schrödinger suite of programs to account for likely adapted fit effects. During the initial Glide docking of the IFD run, the van der Waals radii of nonpolar atoms were scaled by a factor of 0.8, while I133, W224, and D309 were mutated into alanine. At the end of this step, 20 poses were retained, and residues 133, 224, and 309 were mutated back into the original amino acids and optimized along with the residues within 5 Å of the docked pose, to reach the closest energy minimum. This is the central engine of IFD workflows that allows first a comfortable allocation of the ligand within a wider active site and then let the original side chains adapt to the generated pose. At this stage, the ligands were docked back into the rigid induced protein structure and ranked accordingly to the IFDScore, which is a sum of the SP score from the redocking and 5% of the Prime energy from the refinement calculation.

AUTHOR INFORMATION

Corresponding Author

*Tel: ++39-0805442782. Fax: ++39-0805442230. E-mail: carotti@farmchim.uniba.it.

ACKNOWLEDGMENT

We thank the Università degli Studi di Bari "Aldo Moro" and the Fonds der Chemischen Industrie, respectively, for financial support. We also thank Prof. Saverio Cellamare (Dipartimento Farmacochimico, Università degli Studi di Bari "Aldo Moro", Italy) for the development of chiral HPLC analyses.

ABBREVIATIONS USED

ER, estrogen receptor; CYP, cytochrome P450; AR, aromatase; ARI, aromatase inhibitor; SAFIR, structure–affinity relationship; SERM, selective estrogen receptor modulators; HER2, human epidermal growth factor receptor 2; hmAb, human monoclonal antibody

REFERENCES

- (1) Amir, E.; Freedman, O. C.; Seruga, B.; Evans, D. G. Assessing women at high risk of breast cancer: A review of risk assessment models. *J. Natl. Cancer Inst.* **2010**, *102*, 680–691.
- (2) Grodin, J. M.; Siiteri, P. K.; MacDonald, P. C. Source of estrogen production in postmenopausal women. *J. Clin. Endocrinol. Metab.* **1973**, *36*, 207–214.
- (3) O'Neill, J. S.; Elton, R. A.; Miller, W. R. Aromatase activity in adipose tissue from breast quadrants: A link with tumour site. *Br. Med. J. (Clin. Res. Ed.)* **1988**, *296*, 741–743.

- (4) Thorsen, T.; Tangen, M.; Stoa, K. F. Concentration of endogenous oestradiol as related to oestradiol receptor sites in breast tumor cytosol. *Eur. J. Cancer Clin. Oncol.* **1982**, *18*, 333–337.
- (5) Blankenstein, M. A.; Szymczak, J.; Daroszewski, J.; Milewicz, A.; Thijssen, J. H. Estrogens in plasma and fatty tissue from breast cancer patients and women undergoing surgery for non-oncological reasons. *Gynecol. Endocrinol.* **1992**, *6*, 13–17.
- (6) Banting, L.; Nicholls, P. J.; Shaw, M. A.; Smith, H. J. Recent developments in aromatase inhibition as a potential treatment for oestrogen-dependent breast cancer. *Prog. Med. Chem.* **1989**, *26*, 253–298.
- (7) Lonard, D. M.; Smith, C. L. Molecular perspectives on selective estrogen receptor modulators (SERMs): Progress in understanding their tissue-specific agonist and antagonist actions. *Steroids* **2002**, *67*, 15–24.
- (8) Park, W. C.; Jordan, V. C. Selective estrogen receptor modulators (SERMs) and their roles in breast cancer prevention. *Trends Mol. Med.* **2002**, *8*, 82–88.
- (9) Vogel, V. G.; Costantino, J. P.; Wickerham, D. L.; Cronin, W. M.; Cecchini, R. S.; Atkins, J. N.; Bevers, T. B.; Fehrenbacher, L.; Pajon, E. R., Jr.; Wade, J. L., 3rd; Robidoux, A.; Margolese, R. G.; James, J.; Lippman, S. M.; Runowicz, C. D.; Ganz, P. A.; Reis, S. E.; McCaskill-Stevens, W.; Ford, L. G.; Jordan, V. C.; Wolmark, N. Effects of tamoxifen vs raloxifene on the risk of developing invasive breast cancer and other disease outcomes: the NSABP Study of Tamoxifen and Raloxifene (STAR) P-2 trial. *J. Am. Med. Assoc.* **2006**, *295*, 2727–2741.
- (10) Fisher, B.; Costantino, J. P.; Redmond, C. K.; Fisher, E. R.; Wickerham, D. L.; Cronin, W. M. Endometrial cancer in tamoxifen-treated breast cancer patients: Findings from the National Surgical Adjuvant Breast and Bowel Project (NSABP) B-14. *J. Natl. Cancer Inst.* **1994**, *86*, 527–537.
- (11) Jordan, V. C. Tamoxifen: Toxicities and drug resistance during the treatment and prevention of breast cancer. *Annu. Rev. Pharmacol. Toxicol.* **1995**, *35*, 195–211.
- (12) Silverman, S. L. New Selective Estrogen Receptor Modulators (SERMs) in Development. *Curr. Osteoporosis Rep.* **2010**, *8*, 151–153.
- (13) Baum, M.; Buzdar, A. U.; Cuzick, J.; Forbes, J.; Houghton, J.; Klijn, J. G. M.; Sahmoud, T.; Grp, A. T. Anastrozole alone or in combination with tamoxifen versus tamoxifen alone for adjuvant treatment of postmenopausal women with early breast cancer: First results of the ATAC randomised trial. *Lancet* **2002**, *359*, 2131–2139.
- (14) Thompson, E. A., Jr.; Siiteri, P. K. Utilization of oxygen and reduced nicotinamide adenine dinucleotide phosphate by human placental microsomes during aromatization of androstenedione. *J. Biol. Chem.* **1974**, *249*, 5364–5372.
- (15) Simpson, E. R.; Mahendroo, M. S.; Means, G. D.; Kilgore, M. W.; Hinshelwood, M. M.; Graham-Lorence, S.; Amarneh, B.; Ito, Y.; Fisher, C. R.; Michael, M. D.; Mendelson, C. R.; Bulun, S. E. Aromatase cytochrome P450, the enzyme responsible for estrogen biosynthesis. *Endocr. Rev.* **1994**, *15*, 342–355.
- (16) Akhtar, M.; Calder, M. R.; Corina, D. L.; Wright, J. N. Mechanistic studies on C-19 demethylation in oestrogen biosynthesis. *Biochem. J.* **1982**, *201*, 569–580.
- (17) Akhtar, M.; Njar, V. C.; Wright, J. N. Mechanistic studies on aromatase and related C-C bond cleaving P-450 enzymes. *J. Steroid Biochem. Mol. Biol.* **1993**, *44*, 375–387.
- (18) Eisen, A.; Trudeau, M.; Shelley, W.; Messersmith, H.; Pritchard, K. I. Aromatase inhibitors in adjuvant therapy for hormone receptor positive breast cancer: A systematic review. *Cancer Treat. Rev.* **2008**, *34*, 157–174.
- (19) Mokbel, K. The evolving role of aromatase inhibitors in breast cancer. *Int. J. Clin. Oncol.* **2002**, *7*, 279–283.
- (20) Wong, Z. W.; Ellis, M. J. First-line endocrine treatment of breast cancer: Aromatase inhibitor or antioestrogen?. *Br. J. Cancer* **2004**, *90*, 20–25.
- (21) (a) Milla-Santos, A.; Milla, L.; Portella, J.; Rallo, L.; Pons, M.; Rodes, E.; Casanovas, J.; Puig-Gali, M. Anastrozole versus tamoxifen as first-line therapy in postmenopausal patients with hormone-dependent advanced breast cancer: a prospective, randomized, phase III study. *Am. J. Clin. Oncol.* **2003**, *26*, 317–322. (b) Nabholz, J. M.; Mouret-Reynier, M. A.; Durando, X.; Van Praagh, I.; Al-Sukhun, S.; Ferriere, J. P.; Chollet, P. Comparative Review of Anastrozole, Letrozole and Exemestane in the management of early breast cancer. *Expert Opin. Pharmacother.* **2009**, *10*, 1435–1447.
- (22) Le Borgne, M.; Marchand, P.; Duflos, M.; Delevoye-Seiller, B.; Piessard-Robert, S.; Le Baut, G.; Hartmann, R. W.; Palzer, M. Synthesis and in vitro evaluation of 3-(1-azolylmethyl)-1H-indoles and 3-(1-azoly-1-phenylmethyl)-1H-indoles as inhibitors of P450 arom. *Arch. Pharm. (Weinheim)* **1997**, *330*, 141–145.
- (23) Leze, M. P.; Paluszczak, A.; Hartmann, R. W.; Le Borgne, M. Synthesis of 6- or 4-functionalized indoles via a reductive cyclization approach and evaluation as aromatase inhibitors. *Bioorg. Med. Chem. Lett.* **2008**, *18*, 4713–4715.
- (24) Arora, A.; Potter, J. F. Aromatase inhibitors: Current indications and future prospects for treatment of postmenopausal breast cancer. *J. Am. Geriatr. Soc.* **2004**, *52*, 611–616.
- (25) Gobbi, S.; Cavalli, A.; Rampa, A.; Belluti, F.; Piazzini, L.; Paluszczak, A.; Hartmann, R. W.; Recanatini, M.; Bisi, A. Lead optimization providing a series of flavone derivatives as potent nonsteroidal inhibitors of the cytochrome P450 aromatase enzyme. *J. Med. Chem.* **2006**, *49*, 4777–4780.
- (26) Goss, P. E. Risks versus benefits in the clinical application of aromatase inhibitors. *Endocr. Relat. Cancer* **1999**, *6*, 325–332.
- (27) Gobbi, S.; Cavalli, A.; Negri, M.; Schewe, K. E.; Belluti, F.; Piazzini, L.; Hartmann, R. W.; Recanatini, M.; Bisi, A. Imidazolymethylbenzophenones as highly potent aromatase inhibitors. *J. Med. Chem.* **2007**, *50*, 3420–3422.
- (28) Saberi, M. R.; Vinh, T. K.; Yee, S. W.; Griffiths, B. J.; Evans, P. J.; Simons, C. Potent CYP19 (aromatase) 1-[(benzofuran-2-yl)-(phenylmethyl)pyridine, -imidazole, and -triazole inhibitors: Synthesis and biological evaluation. *J. Med. Chem.* **2006**, *49*, 1016–1022.
- (29) Gobbi, S.; Zimmer, C.; Belluti, F.; Rampa, A.; Hartmann, R. W.; Recanatini, M.; Bisi, A. Novel highly potent and selective nonsteroidal aromatase inhibitors: Synthesis, biological evaluation and structure-activity relationships investigation. *J. Med. Chem.* **2010**, *53*, 5347–5351.
- (30) Leonetti, F.; Favia, A.; Rao, A.; Aliano, R.; Paluszczak, A.; Hartmann, R. W.; Carotti, A. Design, synthesis, and 3D QSAR of novel potent and selective aromatase inhibitors. *J. Med. Chem.* **2004**, *47*, 6792–6803.
- (31) Berman, H.; Henrick, K.; Nakamura, H. Announcing the worldwide Protein Data Bank. *Nat. Struct. Biol.* **2003**, *10*, 980.
- (32) Favia, A. D.; Cavalli, A.; Masetti, M.; Carotti, A.; Recanatini, M. Three-dimensional model of the human aromatase enzyme and density functional parameterization of the iron-containing protoporphyrin IX for a molecular dynamics study of heme-cysteinato cytochromes. *Proteins* **2006**, *62*, 1074–1087.
- (33) Neves, M. A.; Dinis, T. C.; Colombo, G.; Sa e Melo, M. L. Fast three dimensional pharmacophore virtual screening of new potent nonsteroid aromatase inhibitors. *J. Med. Chem.* **2009**, *52*, 143–150.
- (34) Castellano, S.; Stefancich, G.; Ragno, R.; Schewe, K.; Santoriello, M.; Caroli, A.; Hartmann, R. W.; Sbardella, G. CYP19 (aromatase): Exploring the scaffold flexibility for novel selective inhibitors. *Bioorg. Med. Chem.* **2008**, *16*, 8349–8358.
- (35) Baston, E.; Leroux, F. R. Inhibitors of steroidal cytochrome P450 enzymes as targets for drug development. *Recent Pat. Anticancer Drug Discovery* **2007**, *2*, 31–58.
- (36) Zhuang, Y.; Wachall, B. G.; Hartmann, R. W. Novel imidazolyl and triazolyl substituted biphenyl compounds: Synthesis and evaluation as nonsteroidal inhibitors of human 17 α -hydroxylase/C17, 20-lyase (P450 17). *Bioorg. Med. Chem.* **2000**, *8*, 1245–1252.
- (37) Leroux, F. H. T.; Charrière, C.; Scopelliti, R.; Hartmann, R. W. N-(4-Biphenylmethyl)imidazoles as potential therapeutics for the treatment of prostate cancer: metabolic robustness due to fluorine substitution?. *Helv. Chim. Acta* **2003**, *86*, 2671–2686.
- (38) Ghosh, D.; Griswold, J.; Erman, M.; Pangborn, W. Structural basis for androgen specificity and oestrogen synthesis in human aromatase. *Nature* **2009**, *457*, 219–223.
- (39) Ghosh, D.; Griswold, J.; Erman, M.; Pangborn, W. X-ray structure of human aromatase reveals an androgen-specific active site. *J. Steroid Biochem. Mol. Biol.* **2010**, *118*, 197–202.

- (40) Pisani, L.; Muncipinto, G.; Miscioscia, T. F.; Nicolotti, O.; Leonetti, F.; Catto, M.; Caccia, C.; Salvati, P.; Soto-Otero, R.; Mendez-Alvarez, E.; Passeleu, C.; Carotti, A. Discovery of a novel class of potent coumarin monoamine oxidase B inhibitors: Development and biopharmacological profiling of 7-[(3-chlorobenzyl)oxy]-4-[(methylamino)methyl]-2H-chromen-2-one methanesulfonate (NW-1772) as a highly potent, selective, reversible, and orally active monoamine oxidase B inhibitor. *J. Med. Chem.* **2009**, *52*, 6685–6706.
- (41) Evans, D. A.; Katz, J. L.; West, T. R. Synthesis of diaryl ethers through the copper-promoted arylation of phenols with arylboronic acids. An expedient synthesis of thyroxine. *Tetrahedron Lett.* **1998**, *39*, 2937–2940.
- (42) Atkins, R. L.; Bliss, D. E. Substituted coumarins and azocoumarins. Synthesis and fluorescent properties. *J. Org. Chem.* **1978**, *43*, 1975–1981.
- (43) Chan, D. M. T.; Monaco, K. L.; Wang, R. P.; Winters, M. P. New N- and O-arylations with phenylboronic acids and cupric acetate. *Tetrahedron Lett.* **1998**, *39*, 2933–2936.
- (44) Kotwani, N. G.; Sethna, S. M.; Advani, G. D. Pechmann condensation of phenols with ethyl γ -phenylacetoacetate. *J. Univ. Bombay, Sci.: Phys. Sci., Math., Biol. Sci. Med.* **1942**, *10*, 143–147.
- (45) Selwood, D. L.; Brummell, D. G.; Budworth, J.; Burtin, G. E.; Campbell, R. O.; Chana, S. S.; Charles, I. G.; Fernandez, P. A.; Glen, R. C.; Goggin, M. C.; Hobbs, A. J.; Kling, M. R.; Liu, Q.; Madge, D. J.; Meillerais, S.; Powell, K. L.; Reynolds, K.; Spacey, G. D.; Stables, J. N.; Tatlock, M. A.; Wheeler, K. A.; Wishart, G.; Woo, C. K. Synthesis and biological evaluation of novel pyrazoles and indazoles as activators of the nitric oxide receptor, soluble guanylate cyclase. *J. Med. Chem.* **2001**, *44*, 78–93.
- (46) Britto, N.; Gore, V. G.; Mali, R. S.; Ranade, A. C. A Convenient synthesis of 3-benzyl, 3-benzyl-4-substituted coumarins and their benzo derivatives. *Synth. Commun.* **1989**, *19*, 1899–1910.
- (47) Hartmann, R. W.; Batzl, C. Aromatase inhibitors. Synthesis and evaluation of mammary tumor inhibiting activity of 3-alkylated 3-(4-aminophenyl)piperidine-2,6-diones. *J. Med. Chem.* **1986**, *29*, 1362–1369.
- (48) Hutschenreuter, T. U.; Ehmer, P. B.; Hartmann, R. W. Synthesis of hydroxy derivatives of highly potent non-steroidal CYP17 inhibitors as potential metabolites and evaluation of their activity by a non cellular assay using recombinant human enzyme. *J. Enzyme Inhib. Med. Chem.* **2004**, *19*, 17–32.
- (49) Ehmer, P. B.; Jose, J.; Hartmann, R. W. Development of a simple and rapid assay for the evaluation of inhibitors of human 17 α -hydroxylase/C(17,20)-lyase (P450c17) by coexpression of P450c17 with NADPH-cytochrome-P450-reductase in *Escherichia coli*. *J. Steroid Biochem. Mol. Biol.* **2000**, *75*, 57–63.
- (50) Hille, U. E.; Zimmer, C.; Vock, C. A.; Hartmann, R. W. First selective CYP11B1 inhibitors for the treatment of cortisol dependent diseases. *ACS Med. Chem. Lett.* **2011**, *2*, 2–6.
- (51) Lucas, S.; Heim, R.; Negri, M.; Antes, I.; Ries, C.; Schewe, K. E.; Bisi, A.; Gobbi, S.; Hartmann, R. W. Novel aldosterone synthase inhibitors with extended carbocyclic skeleton by a combined ligand-based and structure-based drug design approach. *J. Med. Chem.* **2008**, *51*, 6138–6149.
- (52) Lucas, S.; Heim, R.; Ries, C.; Schewe, K. E.; Birk, B.; Hartmann, R. W. In vivo active aldosterone synthase inhibitors with improved selectivity: Lead optimization providing a series of pyridine substituted 3,4-dihydro-1H-quinolin-2-one derivatives. *J. Med. Chem.* **2008**, *51*, 8077–8087.
- (53) Ulmschneider, S.; Müller-Vieira, U.; Mitrenga, M.; Hartmann, R. W.; Marchais-Oberwinkler, S.; Klein, C. D. P.; Bureik, M.; Bernhardt, R.; Antes, I.; Lengauer, T. Synthesis and evaluation of imidazolylmethylenetetrahydronaphthalenes and imidazolylmethyleneindanes: Potent inhibitors of aldosterone synthase. *J. Med. Chem.* **2005**, *48*, 1796–1805.
- (54) Voets, M.; Antes, I.; Scherer, C.; Müller-Vieira, U.; Biemel, K.; Barassin, C.; Marchais-Oberwinkler, S.; Hartmann, R. W. Heteroaryl substituted naphthalenes and structurally modified derivatives: Selective inhibitors of CYP11B2 for the treatment of congestive heart failure and myocardial fibrosis. *J. Med. Chem.* **2005**, *48*, 6632–6642.
- (55) Hansch, C.; Leo, A.; Hoekman, D. *Exploring QSAR Hydrophobic, Electronic, and Steric Constants*; American Chemical Society: Washington, DC, 1995; Vol. 2.
- (56) D'Acquarica, I.; Gasparrini, F.; Misiti, D.; Villani, C.; Carotti, A.; Cellamare, S.; Muck, S. Direct chromatographic resolution of carnitine and O-acylcarnitine enantiomers on a teicoplanin-bonded chiral stationary phase. *J. Chromatogr. A* **1999**, *857*, 145–155.
- (57) Bottegoni, G.; Kufareva, I.; Totrov, M.; Abagyan, R. Four-dimensional docking: a fast and accurate account of discrete receptor flexibility in ligand docking. *J. Med. Chem.* **2009**, *52*, 397–406.
- (58) Sun, B.; Hoshino, J.; Jermihov, K.; Marler, L.; Pezzuto, J. M.; Mesecar, A. D.; Cushman, M. Design, synthesis, and biological evaluation of resveratrol analogues as aromatase and quinone reductase 2 inhibitors for chemoprevention of cancer. *Bioorg. Med. Chem.* **2010**, *18*, 5352–5366.
- (59) Karkola, S.; Wahala, K. The binding of lignans, flavonoids and coumestrol to CYP450 aromatase: A molecular modelling study. *Mol. Cell. Endocrinol.* **2009**, *301*, 235–244.
- (60) Michaud, L. B.; Buzdar, A. U. Risks and benefits of aromatase inhibitors in postmenopausal breast cancer. *Drug Saf.* **1999**, *21*, 297–309.
- (61) Kennedy, R. O.; Thornes, R. D., Eds. *Coumarins: Biology, Applications and Mode of Actions*; John Wiley and Sons: Chichester, 1997.
- (62) Hirsh, J.; Dalen, J.; Anderson, D. R.; Poller, L.; Bussey, H.; Ansell, J.; Deykin, D. Oral anticoagulants: Mechanism of action, clinical effectiveness, and optimal therapeutic range. *Chest* **2001**, *119*, 8S–21S.
- (63) Pelkonen, O.; Raunio, H.; Rautio, A.; Pasanen, M.; Matti, A. L. The metabolism of coumarin. In *Coumarins: Biology, Applications and Mode of Actions*; O'Kennedy, R., Thornes, R. D., Eds.; John Wiley and Sons: Chichester, 1997.
- (64) Seliger, B. The effects of coumarin and its metabolites on cell growth and development. In *Coumarins: Biology, Applications and Mode of Actions*; O'Kennedy, R., Thornes, R. D., Eds.; John Wiley and Sons: Chichester, 1997.
- (65) Pelkonen, O.; Rautio, A.; Raunio, H.; Pasanen, M. CYP2A6: A human coumarin 7-hydroxylase. *Toxicology* **2000**, *144*, 139–147.
- (66) Touchstone, J. *Advances in Thin-Layer Chromatography*; John Wiley & Sons: New York, 1982.
- (67) Wachall, B. G.; Hector, M.; Zhuang, Y.; Hartmann, R. W. Imidazole substituted biphenyls: A new class of highly potent and in vivo active inhibitors of P450 17 as potential therapeutics for treatment of prostate cancer. *Bioorg. Med. Chem.* **1999**, *7*, 1913–1924.
- (68) Cole, J. C.; Murray, C. W.; Nissink, J. W.; Taylor, R. D.; Taylor, R. Comparing protein-ligand docking programs is difficult. *Proteins* **2005**, *60*, 325–332.
- (69) *MacroModel*, version 9.8; Schrödinger, LLC, New York, NY, 2010.
- (70) *Schrödinger Suite 2009 Induced Fit Docking protocol*; *Glide*, version 5.5, Schrödinger, LLC: New York, NY, 2009; *Prime*, version 2.1; Schrödinger, LLC: New York, NY, 2009.